DEUTSCHES ELEKTRONEN-SYNCHROTRON DESY

DESY 67/14
Mai 1967

Measurements on the Formation, Growth and Recompression of Bubbles in Liquid Hydrogen

by

G. Harigel, G. Horlitz, S. Wolff
Deutsches Elektronen-Synchrotron DESY, Hamburg

2 HAMBURG 52 · NOTKESTIEG 1

Measurements on the Formation, Growth and Recompression of Bubbles in Liquid Hydrogen

by

G. Harigel*, G. Horlitz, S. Wolff
Deutsches Elektronen-Synchrotron DESY, Hamburg

Abstract

In the DESY 85 cm bubble chamber photographs of electron tracks with a momentum of about 2 GeV/c have been taken with a scale-one optical system in bright-field illumination. Growth and recompression of bubbles as well as bubble density have been observed between 24.5 and 28.0°K. Bubble radius as a function of time has been measured at different temperatures, with minimum and static pressures as variable parameters.

A comparison between different theories on the behaviour of bubble growth and recompression is given.

---

*Now in the Study Group for a Big European Bubble Chamber (CERN)

Index

I. Introduction

The knowledge of the growth and collapse of macroscopic bubbles in superheated liquids is of fundamental interest both from a theoretical and an experimental point of view. Not very much experimental work on this subject has been done up to now in large hydrogen bubble chambers.

The purpose of this investigation has been to study these processes in hydrogen in a large temperature and pressure interval and by using different flash delays.

Our experimental results have been compared with calculations based on several theories of bubble growth and recompression. Preliminary results of our experiment are presented here; supplementary measurements will soon be done both in hydrogen and deuterium.

II. Theory

1. Bubble Growth

Several theories exist for the growth of bubbles in superheated liquids, which were originally derived for the case of vapour bubbles in water[1],[2],[3]. As shown by Plesset and Zwick[2], the growth of the radius of a bubble must not be considered from the point of view of hydrodynamics alone. The velocity of bubble growth is limited by the quantity of liquid evaporating at the surface of the bubble. By this evaporation the liquid around the bubble is cooled, and further evaporation depends on the quantity of heat transferred from farther points of the liquid to the neighbourhood of the bubble. Considering this effect, Plesset and Zwick gave the following formula for the velocity of bubble growth:

$$(1) \qquad \frac{dR}{dt} = \left(\frac{3}{\pi}\right)^{1/2} \cdot \frac{k \cdot (T_\ell - T_v)}{L \rho_v D^{1/2}} \cdot \frac{1}{t^{1/2}}$$

with

k = thermal conductivity of the liquid

T_ℓ = temperature of the liquid at large distance from the bubble

T_v = temperature of the vapour inside the bubble

L = latent heat of vaporization

ρ_v = density of the vapour inside the bubble

$D = \frac{k}{c\,\rho_\ell}$ = constant of thermal diffusion

c = specific heat of the liquid

ρ_ℓ = density of the liquid

As long as all parameters in (1) are constant, this formula can be integrated; then it gives the bubble radius as a function of time:

$$(2) \qquad R = A \cdot t^{1/2}$$

with

$$(3) \qquad A = 2 \cdot \left(\frac{3}{\pi}\right)^{1/2} \frac{(k \cdot c \cdot \rho_\ell)^{1/2}}{L \cdot \rho_v} \cdot (T_\ell - T_v)$$

The temperature of the vapour in the bubble is the equilibrium vapour pressure temperature which corresponds to the instantaneous pressure p_d (dynamical pressure) in the liquid. It is assumed that the thermal diffusivity in the vapour is so large that the temperature inside the volume of each bubble can be considered as being uniform and in thermal equilibrium with the liquid at the boundary.

As long as the pressure p_d in the bubble chamber is constant (which normally can be realized only in pressure-stabilized bubble chambers over a certain time interval[4],[5],(2) is a correct solution of (1). In larger bubble chambers it is almost impossible to realize a constant pressure over more than a few milliseconds; consequently p_d is a function of time. Since temperature T_v depends on p_d, all parameters which depend on T_v are a function of time also. Moreover, the temperature in the liquid near the surface of the bubble varies very rapidly with the distance from the boundary. The heat which arrives at the surface of the bubble has to come from the liquid in the neighbourhood of the bubble. The temperature of the liquid in this region defines the values of k, c, and ρ_ℓ. These temperature variations are approximately accounted for by taking the parameters k, c, and ρ_ℓ at a temperature which is the arithmetic mean value between T_v an T_ℓ.

It should be mentioned that L has to be taken at the temperature of the surface of the bubble. For the specific heat one has to take c_p since the pressure must be considered as an independent parameter. Because all parameters in (1) are time-dependent with the exeption of T_ℓ, we have, for the radius,

$$(4) \qquad R = \left(\frac{3}{\pi}\right)^{1/2} \cdot \int_0^t \frac{(k \cdot c_p \cdot \rho_\ell)^{1/2}}{L \cdot \rho_v} \cdot (T_\ell - T_v) \frac{1}{\tau^{1/2}} \, d\tau$$

For the numerical integration of (4) one has to know the measured dynamical pressure in the liquid as a function of time.

In the preceding formulas it was assumed that the bubble rested at the place of its origin, drawing its heat always from the same surrounding volume of liquid during the whole time of its growth. Due to the force of gravitation, bubbles will ascend toward the regions which are still at the initial temperature (T_ℓ). (The ascent

for larger times is shown in Fig. 5a). This leads to corrections which were first calculated by Aleksandrov et al.[6]. They give the expression

$$(5) \quad \frac{dR}{dt} = \frac{1}{2} A \cdot \left(\frac{1}{t} + \frac{2}{9} \frac{U_o}{R} \right)^{1/2}$$

with A as in Formula (3), and

$$(6) \quad U_o = \rho_\ell \cdot g \cdot R^2/3\eta \quad \text{for } R<2\cdot 10^{-2}\text{cm}$$

(Reynold number Re < 1000)

$$(6a) \quad U_o = \sqrt[5]{\frac{4\cdot\rho_v\cdot g\ \sigma^2}{\rho_\ell^2\cdot\alpha\cdot\eta}} \quad \text{for } R>2\cdot 10^{-2}\text{cm} \quad (\text{Re} > 1000)$$

with

g = gravitational acceleration (981 cm/s^2)

η = viscosity of the liquid

σ = surface tension of the liquid

$\alpha = 12\pi$*

2. Recompression

Different theoretical approaches have been made for the recompression process on the assumptions that this process is controlled

a) by heat transport alone, [6], [7]

b) by inertial forces alone, [8]

c) by a simultaneous contribution of both effects.

Rough numerical calculations give a reasonable agreement with our first preliminary measurements under the assumption that the first effect is mainly responsible for recompression at those overpressures which have been used up to now in our bubble chamber. Ascent of bubbles plays an important part in the recompression process. The total time for collapse is much longer than that for growth. Moreover, the recompression process starts with big bubbles which have a high velocity of ascent. In Fig. 5a

*The factor α is not explained in the paper of Aleksandrov et al. (there was only a translation available). Other authors (e.g., [15]) give for α the value used here.

one can see that each bubble has a schlieren tail which marks its path of ascent. From this tail one can estimate the velocity of the bubble, which is in rough agreement with U_o, used in (6) and (6a).

Formulas have been derived by Aleksandrov et al.[6] for two conditions:

For 10^{-3} cm < R < $2 \cdot 10^{-2}$ cm they find

$$(7) \qquad t = \sqrt{\frac{18\pi}{g}} \cdot \sqrt{\eta} \, \frac{L \cdot \rho_v}{\sqrt{k} \cdot \rho_\ell \cdot \sqrt{c_p} \cdot (T_v - T_\ell)} \cdot \sqrt{R}$$

For $R > 2 \cdot 10^{-2}$ cm they find

$$(8) \qquad t = \sqrt{\frac{2\pi}{3}} \cdot \frac{1}{\sqrt{U_o}} \, \frac{L \cdot \rho_v}{\sqrt{k \cdot \rho_\ell \cdot c_p} \cdot (T_v - T_\ell)} \, (R^{3/2} - R'^{3/2}) + t'$$

with

$$U_o = \frac{\rho_\ell \cdot g \cdot R^2}{3\eta} \quad \text{for Reynold numbers Re < 1000}$$

$$U_o = \sqrt[5]{\frac{4 \cdot \rho_v \cdot g \cdot \sigma^2}{\rho_\ell^2 \cdot \alpha \cdot \eta}} \quad \text{for Re > 1000}$$

$R' = 2 \cdot 10^{-2}$ cm

t' = calculated from (7) with $R = R'$

σ = suface tension of the liquid

$\alpha = 12\pi$

For more precise calculations one has to take into account the variation of parameters with temperature, as has been done in the case of bubble growth.

III. Experimental Arrangement and Measurement Procedure

1. Bubble Chamber

For the experiments described below, we have used the 85 x 40 x 40 cm DESY hydrogen bubble chamber. The total illuminated volume is about 110 liters, and the total volume inside the chamber is about 220 liters.

2. Optical Arrangement

The DESY bubble chamber is equipped with 3 cameras and one television camera. The 3 cameras are normally used with lenses of 80 mm focal length (Schneider COMPONON), with the aperture set at F = 32. One of the cameras was removed to make possible the use of a telephoto lens with a focal length of 800 mm (RUBICA with a focal length doubling system TELEMAC VARIO 2 x), and an effective aperture of about 1:30. Fig. 1 shows the relative position of cameras, bubble chamber, and illuminating system.

The television camera uses a zoom lens (Voigtländer Zoomar Mark IV) with a variable focal length between 20 and 240 mm[9]. The adjustment of focus, scale and aperture can be controlled electrically. The optical resolution on the television screen is comparable with the resolution on the film (Fig. 3). For cameras 1 and 3 the visible part of the chamber is the entire illuminated volume of hydrogen, for the television camera it is about 75 per cent of it, and for the telephoto camera it is a spot of about 3 cm diameter. The focal depth is the total depth of the chamber for the normal cameras and about 3 cm for the telephoto camera.

In general the bubble-chamber illuminating system is designed for dark field illumination. Preliminary experiments with the telephoto camera have given better results in bright field illumination. Therefore, all pictures made with this camera have been taken with the flash focussed into the camera lens. Illumination has been done with a linear flash tube (Edgerton, Germershausen & Grier FX 45, length 175 mm). The flash for the telephoto camera was screened by a circular diaphragm of 10 mm diameter. Between flash and bubble chamber a filter was inserted having maximum transmission at 430 nm and a half width of 34 nm.

At normal flash power of about 130 Joules the half width of the light pulse is about 100 /us. For bright field illumination this was reduced to about 10 Joules and 10 /us.

For the normal cameras we used Adox track chamber film (BCF-LL, unsensibilized, 17/10 DIN). For bright field illumination we had to choose a film with higher sinsitivity (SCF Supertyp A, panchromatic, 24/10 DIN). Fig. 2 shows a comparison between photographs made with the normal cameras and photographs made with the telephoto camera.

3. Measurement of Parameters

a) Temperature

The Temperature in the bubble chamber has been measured with three vapour pressure thermometers filled with hydrogen. One of them was placed at the bottom of the bubble chamber, the second one at the upper limit of the visible volume and the third one near the piston. Temperature control has been performed with the second thermometer. Its reading was also taken as the nominal temperature of the liquid. The vapour pressure of this thermometer was measured by means of an electrical pressure transmitter with an overall accuracy of about 20 p/cm^2. The signal of the pressure transducer was displayed on a digital voltmeter. As the thermometers had to be refilled several times during the run, the ortho-para composition of the hydrogen inside the thermometer was not known. Therefore the variation of vapour pressure vs. para concentration had to be neglected; the maximum error introduced by this did not exceed 0.1 ^{o}K between 24 ^{o}K and 28 ^{o}K. The statistical variations in temperature have been ovserved to remain within 0.05 ^{o}K. The temperature gradient across the region of interest did not exceed 0.005 $^{o}K/cm$, which corresponds to about 0.02 ^{o}K over the region where bubbles have been measured.

b) Static Pressure

The static pressure, which was maintained by a gas regulating valve system being connected to the cylinder volume above the piston, was measured by means of a high precision manometer with an accuracy of 0.05 kp/cm^2.

c) Dynamic Pressure

The pressure change (dynamic pressure) during the expansion cycle was determined with a piezoelectric quartz (Kistler, Type 410 A) which was mounted at the bottom of the chamber. The amplified signal was displayed on an oscilloscope and photographed. Fig. 4 shows a typical pressure curve. The calibration factor of the gauge must be considered as preliminary. At present, the overall precision is of the order of about ± 0.1 kp/cm^2.

d) Piston Movement (Expansion Ratio)

The expansion was performed by the movement of a piston. The maximum piston movement is constructionally limited to 30 mm. The change in volume is 0.765 liters per cm displacement of the piston, which corresponds to an expansion value of 0.347 per cent per cm. The piston movement has been measured by means of an optical device consisting of a grid attached to the piston, a light source and a photocell. The grid interrupted the light beam every 0.5 mm, and the pulses from the photodiode due to these interruptions were counted.

Simultaneously the piston movement was measured by means of a magnetic transducer, the signal of which was displayed on an oscilloscope.

e) Repetition Rate

The repetition rate for the piston movement was reduced to 1 expansion per second, in order to make sure that the liquid was always in thermal equilibrium.

f) Timing

The expansion system of the bubble chamber was triggered by a signal from the accelerator, which could be shifted in such a way that the incident particle beam arrived at different times relative to the minimum of the dynamic pressure. The flash was triggered by a second pulse. The delay of this flah trigger relative to the beam injection time could be changed between 10 /us and 999.9 ms.

4. Beam

The chamber was exposed to an electron beam with a momentum of about 2 GeV/c, i.e. minimum ionizing particles with relativistic energy. The burst length was 50 /us, the time jitter of the beam was smaller than 50 /us. The beam profile inside the chamber was about 10 cm in height and 5 cm in depth. The beam has been injected into the chamber at different times relative to the minimum of the dynamic pressure (Fig. 4). The beam intensity was approximately 15-20 electrons per pulse.

5. Determination of Bubble Diameters and Bubble Density

For each combination of parameters (temperature, static pressure, minimum pressure and flash delay) 20 photographs were taken by the telephoto camera (scale 1:1) as well as by the normal cameras (scale approx. 1:15). The diameters of the bubbles were measured on a conventional measuring projector with a resolution of about 0.03 mm. Only sharp bubbles in the center of the frame have been chosen on the 1:1 photos (Fig. 5 shows some typical pictures of bubble growth at 25.0 ^{o}K.

Each measured point in our plots represents the mean value of some 20 bubble radii. The error contained in this value is about ± 0.02 mm for flash delays up to 10 ms. For longer flash delays the shape of the bubbles is no longer circular because of the rapid ascent in the liquid. Consequently the radius is not well defined and the errors become bigger.

Although the experiment was specially designed to measure bubble growth, some measurements of bubble density were done as well. For each parameter combination we counted about 100 bubbles on different tracks. The errors for the measured bubble densities are of the order of 10 %.

IV. Experimental Results

1. Bubble Growth

A summary of all measurements of bubble growth is given in Table I. The temperature has been changed from 24.5 ^{o}K to 28.0 ^{o}K in intervals of

0.5 ^{o}K. The lower limit was given by the properties of our expansion system, which does not allow to reach the minimum pressure which is necessary to make the chamber sensitive at lower temperatures; the experiment will be extended to temperatures above 28 ^{o}K lateron. At each temperature the static pressure p_s and the piston stroke have been changed in certain intervals. This led to different pressure curves. The minima (p_{min}) are indicated in the table. In these measurements the beam was always injected at the time corresponding to p_{min} (see Fig. 4). The time of bubble growth was determined by the delay between injection time and flash trigger. Proceeding on the assumption that, with constant thermodynamic conditions in the liquid, bubble growth always occurs in the same way, we measured, at a fixed flash delay, the diameters of different bubbles and took the mean value of these measurements and then repeated the procedure with another flash delay.

Figs. 6-12 represent the results of these measurements for growth times up to 4 ms. Because of the time dependent pressure it is not possible to fit the experimental points by a pure $t^{1/2}$-law. Empirically we got a better fit by $(A'+B\cdot t)t^{1/2}$. A' corresponds to A in (2), and B represents the time dependence of the parameters in the first approximation. In some cases the curves fitted to the experimental points intersect. This is caused by different shapes of the pressure curves.

Equation (4) has been computed for each set of parameters indicated in Table 1 using the experimental pressure curves. For one case at each temperature, the theoretical and experimental results were compared in Figs. 13-19.
Curve (a) represents the experimental points fitted by $(A'+B\cdot t)t^{1/2}$, (b) is a fit of $A \cdot t^{1/2}$ for all measured points with $t < 1$ ms, (c) is the theoretical curve using Formula (4), and (d) represents a correction for ascending bubbles using Formula (5). Within the errors of our measurements discussed in Chapter III, curve (c) is in reasonalbe agreement with the experimental values. For growth times smaller than 4 ms the influence of ascent seems to be very small.

For the other parameter combinations which are not represented in the figures a comparison with theory is given in Table II. Here $A(p_{min})_{th}$ is calculated from (3) using all parameters corresponding to p_{min}. This can be compared with $A(p_{min})_{exp}$ which one gets from a fit of $A \cdot t^{1/2}$

for $t \leq 1$ ms, where the variation of p can be neglected. Fig. 20 gives the relative differences $\frac{A(p_{min})_{theor.} - A(p_{min})_{exp.}}{A(p_{min})_{theor.}}$.

The points are randomly distributed around zero. No essential systematic deviation could be found.

For practical application it is useful to know the behaviour of A as a function of temperature for a certain constant bubble density (Fig. 21).

2. Bubble Recompression

In the preceding chapter the time of bubble growth has been investigated only up to 4 ms. For larger growth times a comparison between theory and experiment is very difficult. Due to the variation in time of the dynamic pressure one has an overlapping of bubble growth and recompression effects, which cannot easily be separated.

Figs. 22-28 show the behaviour of bubbles from the moment of their production to the time of their complete disappearance. Within our present errors the points measured during the decrease of bubble radius can roughly be represented by a straight line. The time difference between the moment when the dynamic pressure is equal to the static pressure and the moment when this line intersects the time axis, is here defined as the recompression time. The times measured in this manner are summarized in Table IV. They can be compared with the theoretical values calculated from (7) and (8). These values give better agreement with our experiment than calculations omitting the effects of ascent, or calculations in which the inertial forces alone are held responsible for the control of collapse.

3. Bubble Density

In measuring bubble densities one has to consider that for higher densities and larger growth times several neighbouring bubbles will unite to form a single bubble, which leads to smaller values of bubble density.

Fig. 29 demonstrates that at high initial bubble densities the number of bubbles will decrease with time, whereas at lower initial bubble densities this number will remain constant.

In all our measurements of bubble density a flash delay of 0.5 ms has proved to be a reasonable value for obtaining the initial density within the limits of the experimental error.

Fig. 30 shows the usual plot of measured bubble densities in a p-T diagram. For studying bubble formation at different initial pressures, the electrons were injected at different times before the minimum of the dynamic pressure was reached (see Fig. 4). Fig. 31 shows the bubble density as function of the dynamic pressure for several temperatures. Within the limits of error the measured points at each temperature lie on a straight line. The behaviour at very low bubble densities has yet to be investigated; from other measurements in propane[10] and hydrogen[11],[12] one can expect to find a deviation from linearity at very low bubble densities.

V. Conclusions

Our measurements show that, according to the theory of Plesset and Zwick, heat transfer plays the predominant part in the process of bubble growth. If we take into account the time dependence of parameters we find reasonable agreement between calculations and measurements for small growth times. For longer growth times the increasing influence of bubble ascent has to be taken into consideration. At constant bubble densities the velocity of bubble growth increases rapidly with decreasing operating temperature of the chamber. For bubble recompression heat transfer is also predominant, whereas inertial forces seem to be negligible. The ascent of bubbles has been shown to be of great importance in the case of recompression, and a rough agreement with the theoretical predictions by Aleksandrov et al. has been found.

VI. Acknowledgements

We are greatly indebted to Professor M.W. Teucher for his continued interest and encouragement in the course of these investigations. We also thank R. Florent, G. Linser and Professor R.I. Louttit for helpful discussions, the Machine Group for the excellent performance of the synchrotron Dr. E. Lohrmann and H. Meyer and their crew for the installation and operation of the beam. Furthermore we have to thank our bubble chamber team, expecially W. Eschricht, U. Knopf, D. Nowakowski, O. Peters, and W. Stahlschmidt, as well as Miss I. Kurth and R. Lange for the measurements of the film and the drawing of the figures.

References

1. M. Volmer, Kinetik der Phasenbildung, Dresden 1939
2. M.S. Plesset, S.A. Zwick, J. Appl. Phys. 25, 493 (1954)
3. H.K. Foster, N. Zuber, J.Appl. Phys. 25, 474 (1954)
4. E.v. Kuznecov, M.F. Lomanov, G.A. Blinov, Chuan Chen-Niang, Khuan Shen-Nian, Sov. Phys. JETP 4, 773 (1957)
5. B. Hahn, A.W. Knudsen, E. Hugentobler, Nuovo Cimento Suppl. 15, 236-245, (1960)
6. Yu.A. Aleksandrov, G.S. Voronov, N.B. Delone, Pribory i Tekhn. Eksperim. No. 2, 41 (1963)
7. Badier, Blondet, Briandet, Cornic, Delcros, Demoulin, Dupont, Florent, Guibert, Jacob, Maiorana, Maury, Milito, Morize, Rapport CEA-R3144 (CEN-SACLAY, Ecole Polytechnique Paris) (1967)
8. L.W. Florschütz, B.T. Chao, Heat Transfer, 209 (1965)
9. Erfahrungen bei der Verwendung einer Fernsehkamera zur Beobachtung von Blasenkammer-Spuren. DESY - B 1-, 1966. Internal Report, unpublished.
10. P. Kunkel, G. Christenn, M. Scheer, to be published in Z. angew. Phys. (1967)
11. B.N. Fabian, R.L. Place, W.A. Riley, W.H. Sims, V.P. Kenney, Rev. Sci. Instr. 34, 484 (1963)
12. N.N. Biswas, N.M. Cason, I. Derado, V.P. Kenney, J.A. Poirier, W.D. Shephard, and Sr.E.M. Clinton, Proceedings of the International Conference on Instrumentation of High Energy Physics, Stanford (1966)
13. J.E. Jensen, R.B. Stewart, W.A. Tuttle, Selected Cryogenic Data Notebook, Brookhaven National Laboratory BNL 10200 (1967)
14. W.D. Shephard Thermodynamic constants for Para H_2, Ne, and mixtures, Argonne National Laboratory, 8/25/66 unpublished
15. L. Prandtl, Führer durch die Strömungslehre, Braunschweig 1965.

Table I: Thermodynamic parameters

T = temperature of the liquid

p_v = vapour pressure at temperature T

p_{min} = minimum of dynamic pressure during the expansion cycle

p_s = static pressure in the liquid before the expansion ($p_s > p_v$)

Table II: Experimental results (bubble growth, bubble density)

$A(p_{min})_{th}$ = theoretical bubble growth parameter, calculated from (3) under the assumption $p = \text{const} = p_{min}$.

$A(p_{min})_{exp}$ = experimental bubble growth parameter obtained by a fit of the function $A \cdot t^{1/2}$ to the measured points for $k < 1$ ms (variation of p is neglected)

bubble density = number of bubbles per cm in the chamber

Table III: Thermodynamic properties of hydrogen

p_v = vapour pressure[13]

ρ_ℓ = density of the liquid[13]

ρ_v = density of the saturated vapour[13]

k_ℓ = thermal conductivity[13]

c_p = specific heat of the liquid at constant pressure[14]

L = latent heat of vaporization[13]

η = viscosity[13]

σ = surface tension[14]

Table IV: Experimental results (recompression)

p_{over} = overpressure = $p_s - p_v$

R_{max} = maximum radius during expansion cycle

$t(R_{max})_{exp}$ = experimental time for recompression of bubbles having radius R_{max}

R_{p_s} = radius of bubbles at the time when the dynamic pressure becames equal to the static pressure

$t(R_{p_s})_{exp}$ = measured recompression time for bubbles having radius R_{p_s}

$t(R_{p_s})_{th}$ = calculated recompression time (Eq.'s (7), (8)) for bubbles having radius R_{p_s}

Table I Thermodynamic parameters

No	T	p_v	p_{min}	p_s
	^oK	kp/cm^2	kp/cm^2	kp/cm^2
1	24.5	3.0	0.8	3.3
2	24.5	3.0	0.7	3.9
3	24.5	3.0	0.7	3.3
4	25.0	3.3	1.5	5.1
5	25.0	3.3	1.2	4.5
6	25.0	3.3	1.1	3.9
7	25.0	3.3	0.7	3.9
8	25.0	3.3	0.7	3.6
9	25.0	3.3	0.4	3.6
10	25.5	3.7	1.5	5.4
11	25.5	3.7	1.1	4.8
12	25.5	3.7	1.1	4.5
13	26.0	4.1	1.8	5.1
14	26.0	4.1	1.7	4.5
15	26.0	4.1	1.3	6.3
16	26.0	4.1	1.3	5.5
17	26.5	4.5	1.7	6.3
18	26.5	4.5	1.7	5.9
19	26.5	4.5	1.7	5.3
20	27.0	5.0	2.3	5.9
21	27.0	5.0	2.3	5.3
22	27.0	5.0	2.0	6.5
23	28.0	6.0	2.7	6.5
24	28.0	6.0	2.3	6.2

Table II Experimental results (bubble growth, bubble density)

No	T	p_{min}	$A(p_{min})_{th}$	$A(p_{min})_{exp}$	bubble density
	^oK	kp/cm^2	$cm/\sqrt{s}$	$cm/\sqrt{s}$	b/cm
1	24.5	0.8	0.63	0.50	2.7
2	24.5	0.7	0.82	0.71	3.6
3	24.5	0.7	0.82	0.53	2.7
4	25.0	1.5	0.25	0.47	3.9
5	25.0	1.2	0.41	0.54	4.0
6	25.0	1.1	0.46	0.55	4.8
7	25.0	0.7	0.79	0.78	7.5
8	25.0	0.7	0.73	0.92	9.1
9	25.0	0.4	1.90	0.99	10.6
10	25.5	1.5	0.30	0.41	6.7
11	25.5	1.1	0.48	0.53	10.7
12	25.5	1.1	0.49	0.41	8.2
13	26.0	1.8	0.24	0.32	7.3
14	26.0	1.7	0.28	0.31	8.2
15	26.0	1.3	0.47	0.38	9.6
16	26.0	1.3	0.40	0.59	11.3
17	26.5	1.7	0.32	0.25	13.3
18	26.5	1.7	0.41	0.32	14.0
19	26.5	1.7	0.31	0.28	18.0
20	27.0	2.3	0.21	0.24	17.1
21	27.0	2.3	0.20	0.25	20.4
22	27.0	2.0	0.26	0.27	18.5
23	28.0	2.7	0.20	0.24	41
24	28.0	2.3	0.26	0.31	46

Table III Thermodynamic properties of hydrogen

T	p_v	ρ_ℓ	ρ_v	k_ℓ	c_p	L	η	σ
^oK	atm*	gmole/cm^3 $\cdot 10^2$	gmole/cm^3 $\cdot 10^5$	cal/cm s ^oK $\cdot 10^4$	cal/g ^oK	cal/gmole	g/cm s $\cdot 10^6$	g/s^2
15	0.132	3.770	11.04	2.537	1.669	218.03	221.3	2.792
16	0.212	3.726	16.78	2.593	1.769	218.40	197.5	2.627
17	0.325	3.679	24.40	2.649	1.887	218.36	177.7	2.462
18	0.475	3.631	34.20	2.705	2.013	217.85	160.5	2.299
19	0.672	3.580	46.53	2.761	2.140	216.78	147.0	2.136
20	0.922	3.526	61.76	2.817	2.270	215.12	135.4	1.973
21	1.233	3.469	80.30	2.872	2.429	212.76	125.3	1.811
22	1.612	3.409	102.7	2.928	2.589	209.57	116.1	1.651
23	2.069	3.344	129.6	2.984	2.787	205.67	108.1	1.491
24	2.610	3.274	161.5	3.040	2.993	200.81	100.8	1.333
25	3.245	3.199	199.3	3.095	3.243	194.86	93.5	1.175
26	3.981	3.117	244.1	3.151	3.532	187.71	87.2	1.019
27	4.828	3.026	297.6	3.207	3.905	179.01	83.1	0.864
28	5.793	2.925	362.0	3.262	4.433	168.67	79.0	0.711
29	6.886	2.810	440.8	3.318	5.174	155.90	73.5	0.560
30	8.117	2.675	540.1	3.374	6.426	140.15	68.0	0.411

* 1 atm = 1.033 kp/cm^2

Table IV Experimental results (recompression)

No	T	$p_{over} = p_s - p_v$	R_{max}	$t(R_{max})_{exp}$	R_{p_s}	$t(R_{p_s})_{exp}$	$t(R_{p_s})_{th}$
	°K	kp/cm²	mm	ms	mm	ms	ms
1	24.5	0.3	0.40	25	0.17	10	135
2	24.5	0.9	0.41	65	0.31	50	62
3	24.5	0.3	0.38	45	0.26	30	175
4	25.0	1.8	0.24	25	0.07	5	17
5	25.0	1.2	0.27	30	0.13	15	34
6	25.0	0.6	0.31	45	0.22	30	79
7	25.0	0.6	0.39	75	0.32	60	97
8	25.0	0.3	0.45	160	0.43	150	174
9	25.0	0.3	0.47	190	0.41	180	169
10	25.5	1.7	0.23	35	0.12	15	28
11	25.5	1.1	0.28	50	0.22	40	50
12	25.5	0.8	0.26	50	0.17	30	61
13	26.0	1.0	0.19	30	0.09	15	39
14	26.0	0.4	0.20	50	0.16	40	112
15	26.0	2.2	0.18	30	0.03	5	14
16	26.0	1.4	0.24	45	0.18	35	38
17	26.5	1.8	0.19	40	0.13	25	28
18	26.5	1.4	0.20	45	0.15	35	37
19	26.5	0.8	0.21	60	0.19	50	70
20	27.0	1.0	0.17	50	0.13	40	50
21	27.0	0.4	0.16	110	0.15	100	144
22	27.0	1.6	0.17	50	0.13	40	28
23	28.0	0.5	0.19	120	0.16	105	84
24	28.0	0.2	0.24	350	0.22	320	190

Figure captions

Fig. 1 Relative position of cameras, bubble chamber and illuminating system.

Fig. 2 Comparison between bubble photographs taken with different focal length. Original photographs have been enlarged by different factors so that the scale of both types of pictures is identical and equal 2:1.

Fig. 3 Bubble track photographs taken from the television screen. Two different focal lengths of the zooms lens in front of the vidicon have been used. The dimensions of the television screen are 28 cm x 21 cm.

Fig. 4 Typical expansion at 25.0 ^{o}K.

p_s = static pressure in the liquid prior to expansion

p_v = vapour pressure

p_{min} = minimum of dynamic pressure during the expansion cycle.

Fig. 5 Typical photographs of bubble growth at different flash delays. Original photographs have been enlarged by a factor 2. T = 25.0 ^{o}K, p_s = 3.6 kp/cm^2, p_{min} = 0.7 kp/cm^2.

Fig. 5a Typical photographs of bubble growth at different flash delays. Same as Fig. 5 but for longer flash delays. The ascent of bubbles is marked by a schlieren track.

Fig. 6-12 Bubble radius as a function of flash delay. The numbers of the curves correspond to the numbers in Tables I, II, IV, where the other parameters can be found.

Fig. 13-19 Comparison with theory.

Fig. 20 Deviations of measured bubble growth from the theory of Plesset and Zwick.

A_{th} = theoretical bubble growth parameter calculated from (3) under the assumption p = const = p_{min}.

A_{exp} = experimental bubble growth parameter obtained by a fit of function $A \cdot t^{1/2}$ to the measured points for t < 1 ms (variation of p neglected).

The numbers marked at the measured points correspond to the numbers of the curves in Figs. 6-12.

Fig. 21 Rate of bubble growth as a function of temperature for constant bubble densities.
The indicated points have been found by interpolations and extrapolations, plotting the measured values of A vs. bubble density for each temperature.

Fig. 22-28 Bubble radius as a function of flash delay. V denotes the time when the dynamic pressure reaches the vapour pressure.
S denotes the time when the dynamic pressure reaches the static pressure.
The indicated errors represent the r.m.s. error (solid line) and the maximum error (dotted line) respectively.

Fig. 29 Bubble density as a function of growth time.

Fig. 30 Bubble density at various points in a p-T diagram.

Fig. 31 Bubble density as a function of pressure.
p is the instantaneous pressure at the injection time of particles.

Front view

Camera 1

C1

Television Camera

C2

Camera 3

C3

Top view

C2 Telephoto Camera

Telephoto Lens f = 800 mm

Scale

0 500 1000 1500 2000 mm

Camera 2 Telephoto Camera

Magnet Coil

C1/C3

Liquid hydro-gen

Flash 1 120 Joule 100 µs

Flash 2 120 Joule 100 µs

Flash 3 10 Joule 10 µs half width

RELATIVE POSITION
OF CAMERAS, BUBBLE CHAMBER
AND ILLUMINATING SYSTEM

Fig. 1

Fig. 2

Comparison between Bubble Photographs Taken with Different Focal Length

f = 800 mm
bright field illumination

f = 80 mm
dark field illumination

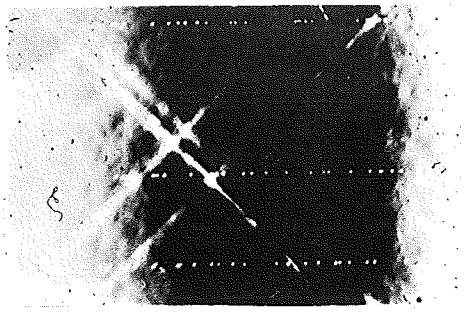

0.1 ms

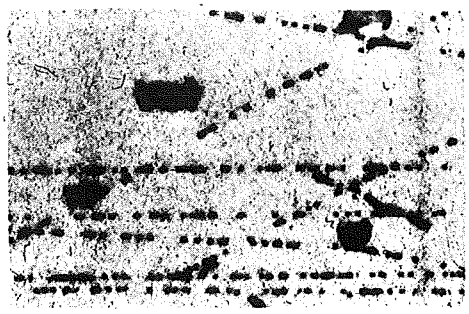

0.1 ms

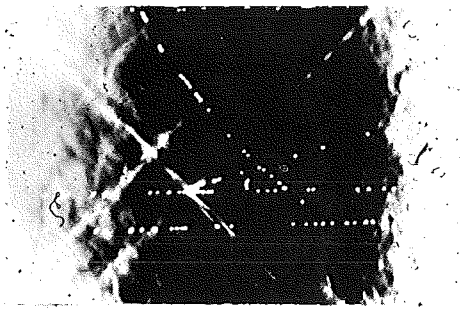

0.2 ms

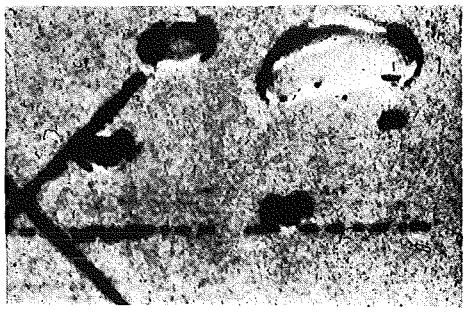

0.2 ms

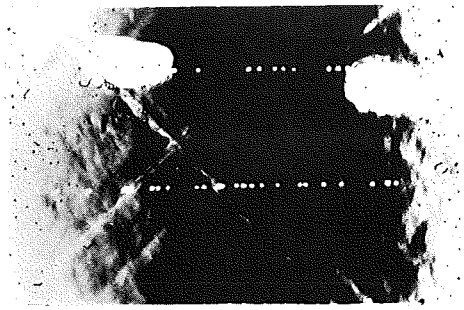

0.4 ms

0.4 ms

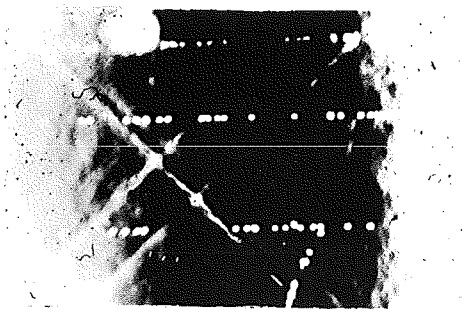

0.8 ms

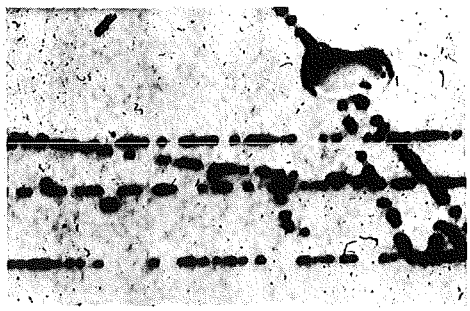

0.8 ms

Fig. 3
Bubble Track Photographs Taken from the Television Screen

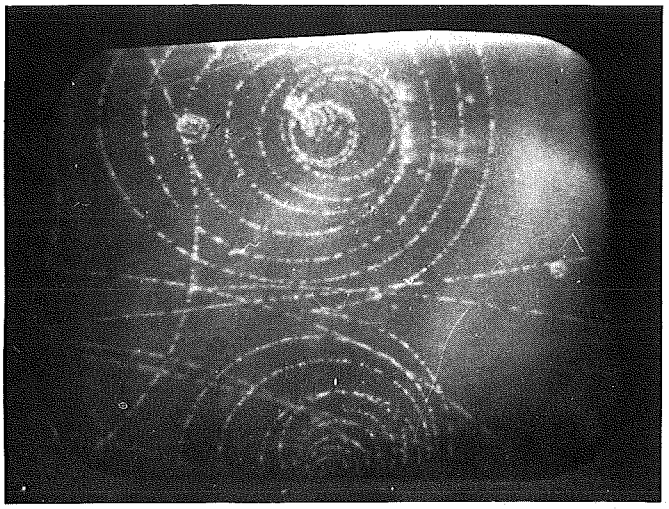

f = 240 mm

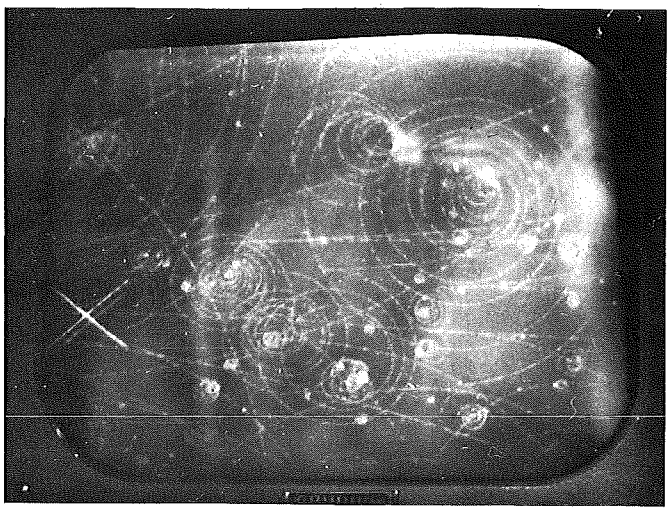

f ≈ 150 mm

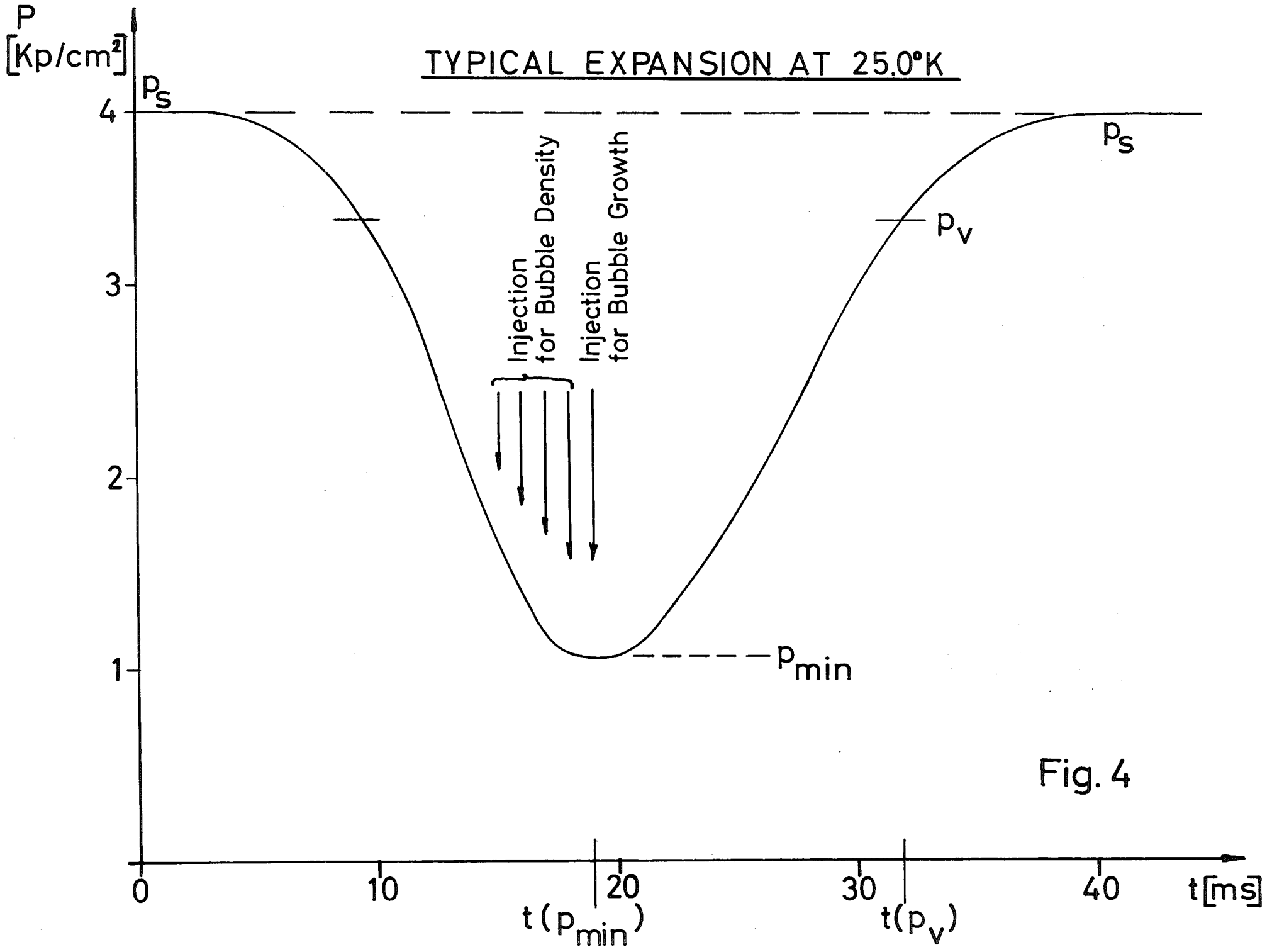
P
[Kp/cm²]
TYPICAL EXPANSION AT 25.0°K
p_s
4
3
2
1
p_s
p_v
Injection for Bubble Density
Injection for Bubble Growth
p_{min}
0
10
20
30
40
t[ms]
$t(p_{min})$
$t(p_v)$

Fig. 4

Fig. 5

Typical Photographs of Bubble Growth at Different Flash Delays

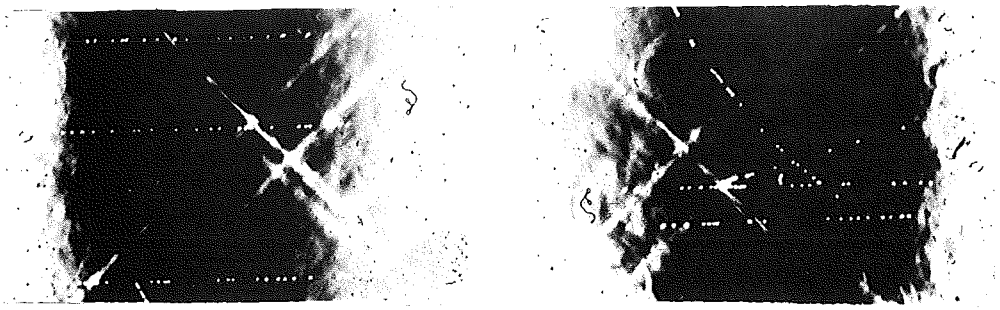

0.1 ms

0.2 ms

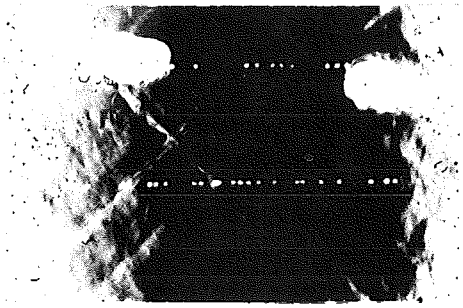

0.4 ms

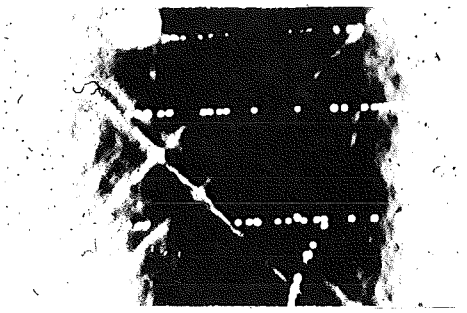

0.8 ms

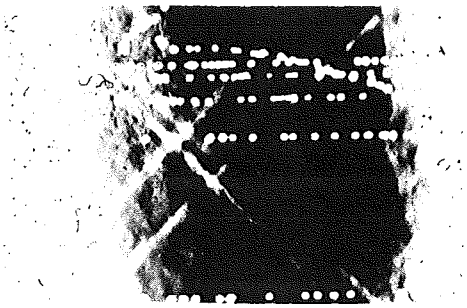

1.0 ms

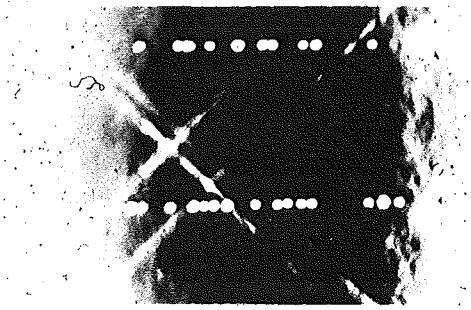

2.0 ms

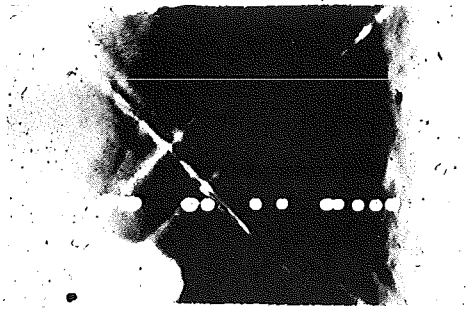

3.0 ms

4.0 ms

Fig. 5a

Typical Photographs of Bubble Growth at Different Flash Delays

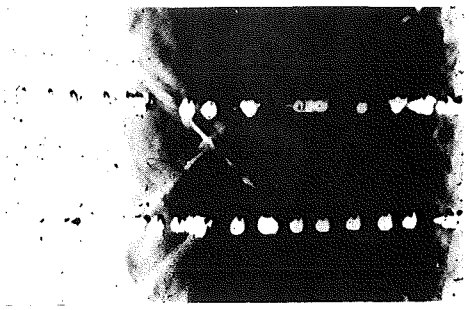

8.0 ms

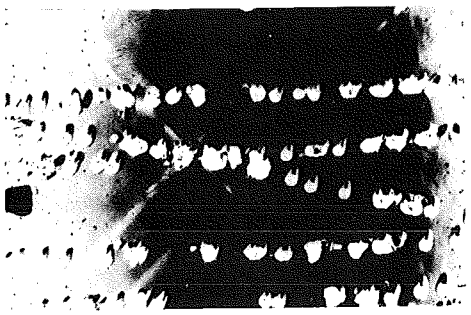

10.0 ms

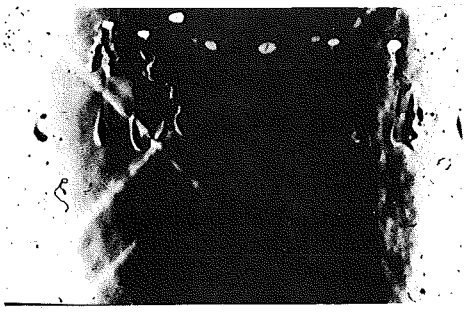

40.0 ms

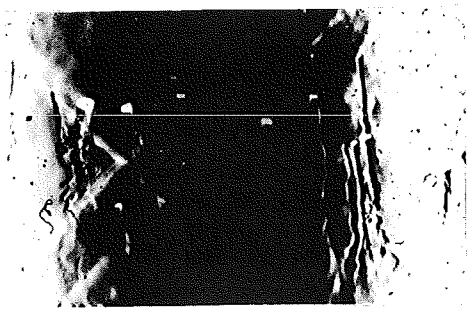

200.0 ms

Fig. 6

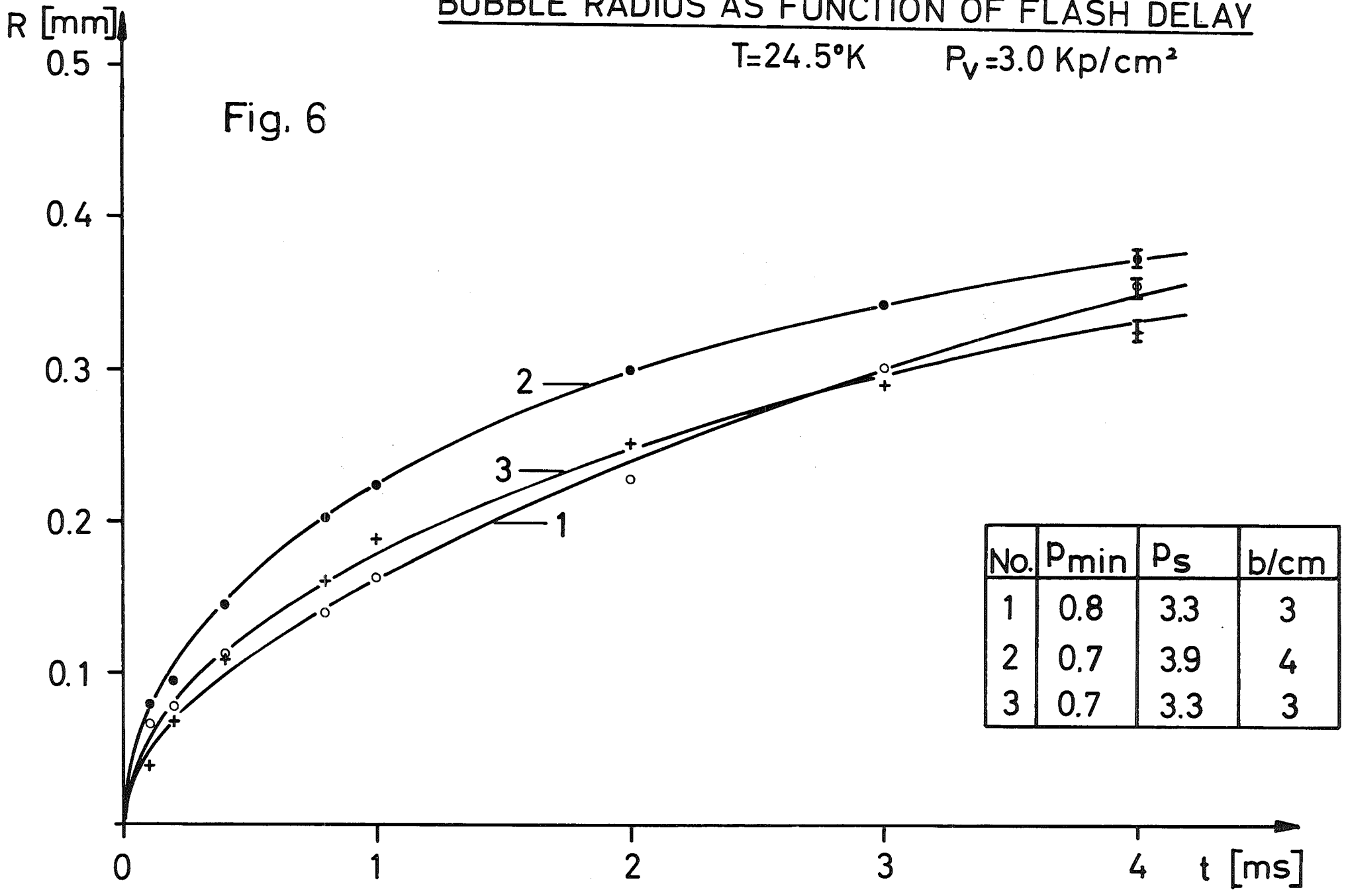

No.	P_{min}	P_s	b/cm
1	0.8	3.3	3
2	0.7	3.9	4
3	0.7	3.3	3

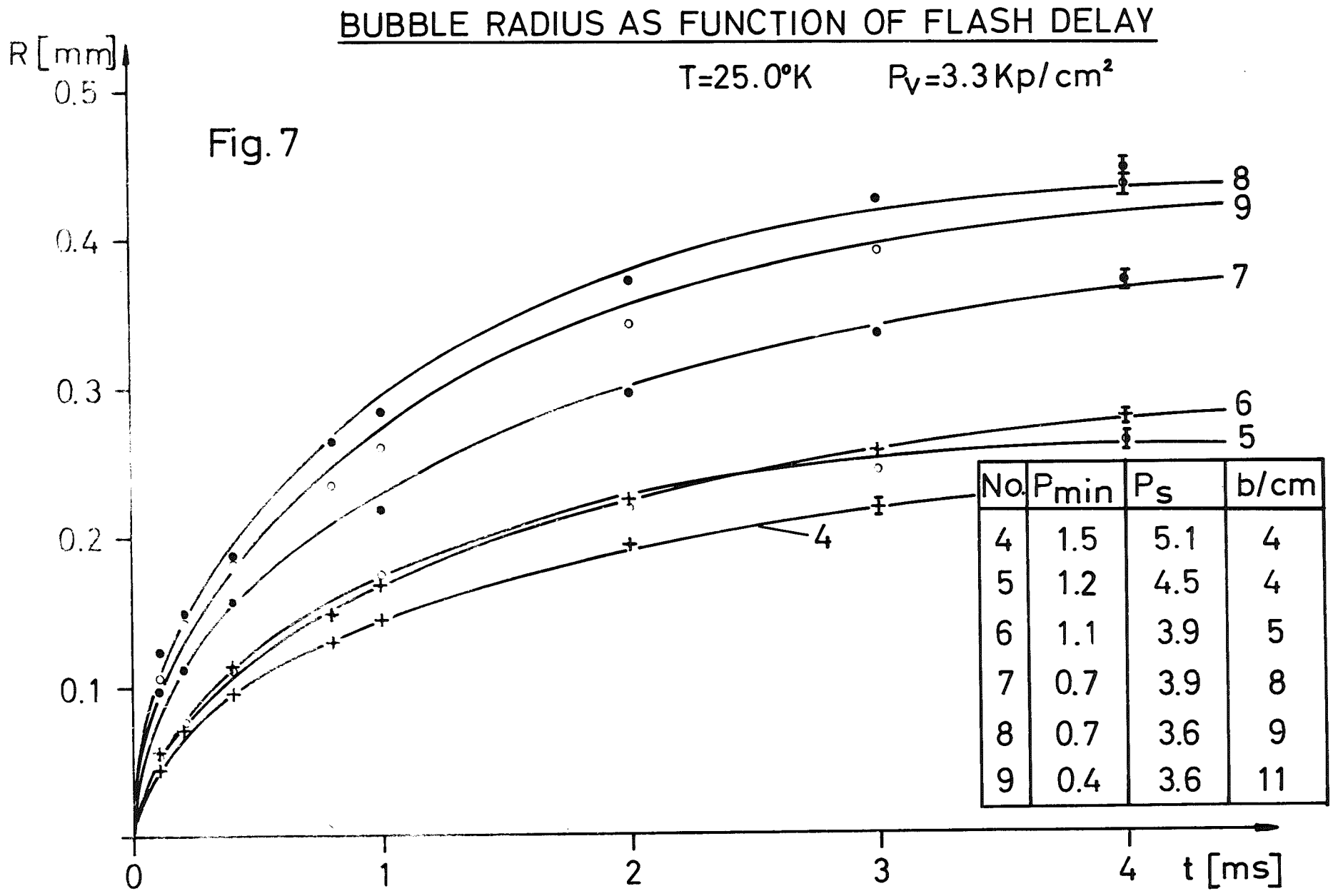
BUBBLE RADIUS AS FUNCTION OF FLASH DELAY
T=25.0°K
P_V=3.3 Kp/cm²
R [mm]
0.5
0.4
0.3
0.2
0.1
0
1
2
3
4
t [ms]
8
9
7
6
5
4
No. | P_{min} | P_s | b/cm
4 | 1.5 | 5.1 | 4
5 | 1.2 | 4.5 | 4
6 | 1.1 | 3.9 | 5
7 | 0.7 | 3.9 | 8
8 | 0.7 | 3.6 | 9
9 | 0.4 | 3.6 | 11

Fig. 7

BUBBLE RADIUS AS FUNCTION OF FLASH DELAY

T=25.5°K $P_V = 3.7$ Kp/cm²

Fig.8

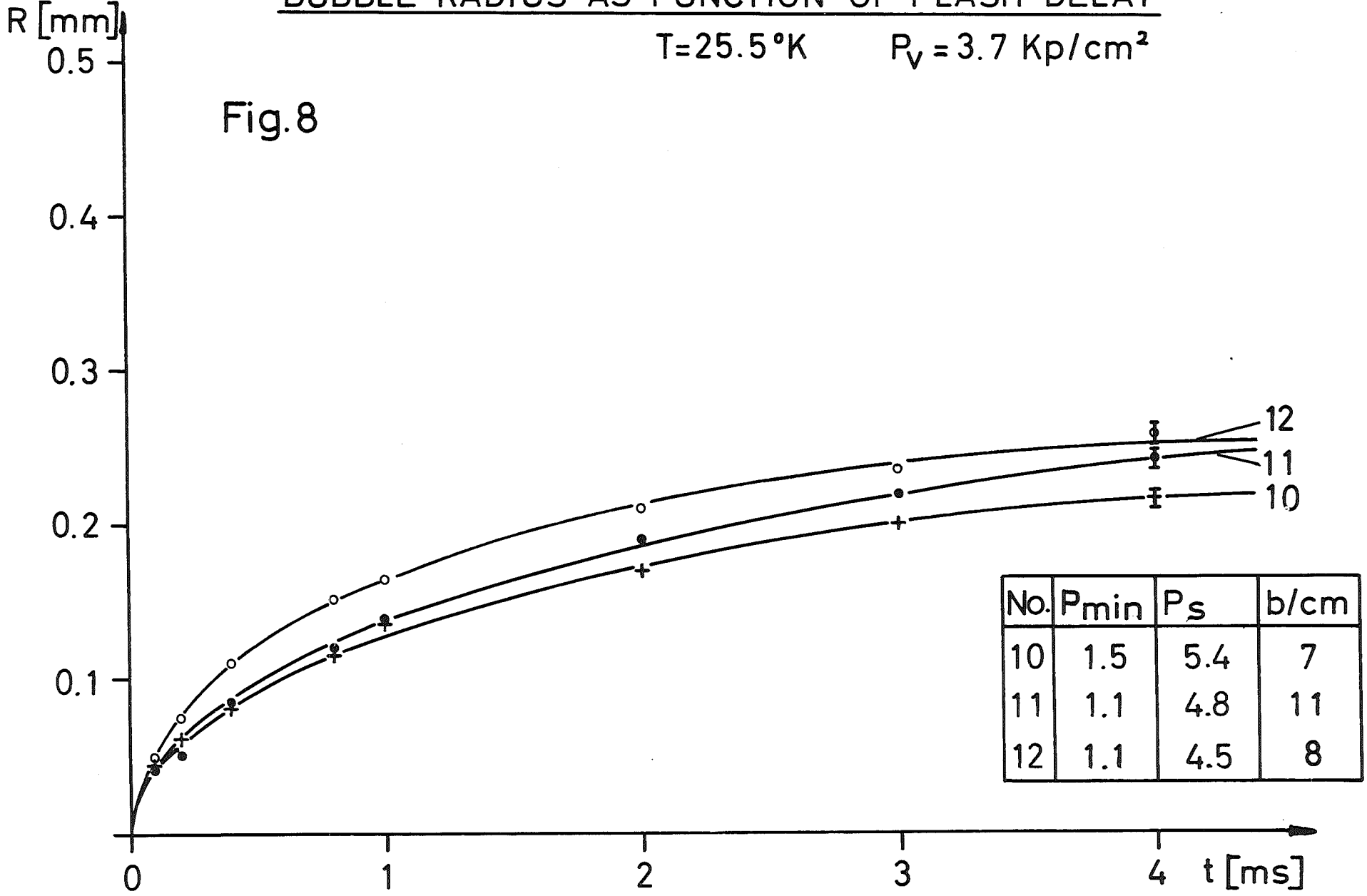

No.	Pmin	Ps	b/cm
10	1.5	5.4	7
11	1.1	4.8	11
12	1.1	4.5	8

BUBBLE RADIUS AS FUNCTION OF FLASH DELAY

T=26.0°K P_v=4.1 Kp/cm²

Fig.9

No.	P_{min}	P_s	b/cm
13	1.8	5.1	7
14	1.7	4.5	8
15	1.3	6.3	10
16	1.3	5.5	11

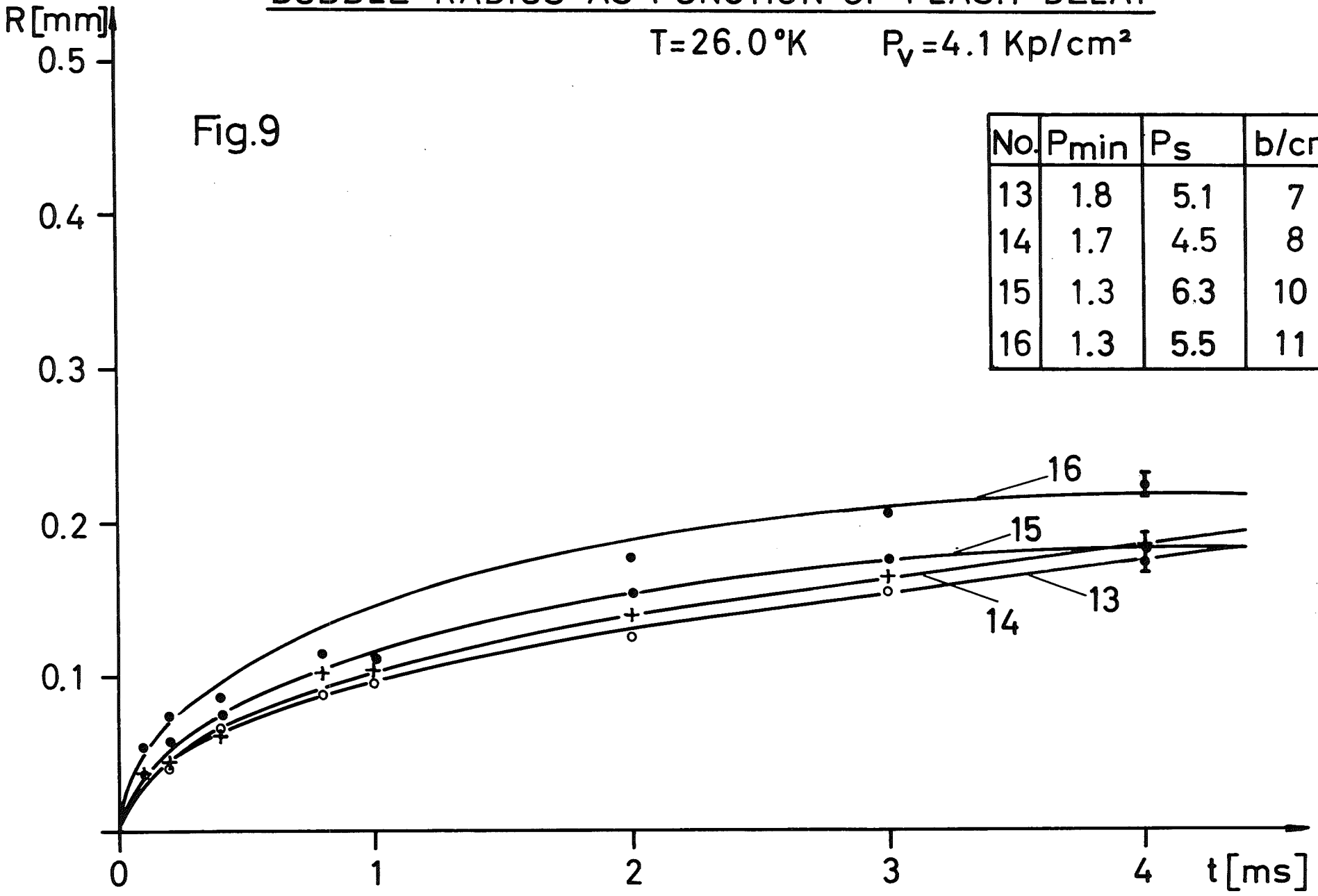

BUBBLE RADIUS AS FUNCTION OF FLASH DELAY

T=26.5 °K P_v = 4.5 Kp/cm²

Fig. 10

No.	P_{min}	P_s	b/cm
17	1.7	6.3	13
18	1.7	5.9	14
19	1.7	5.3	18

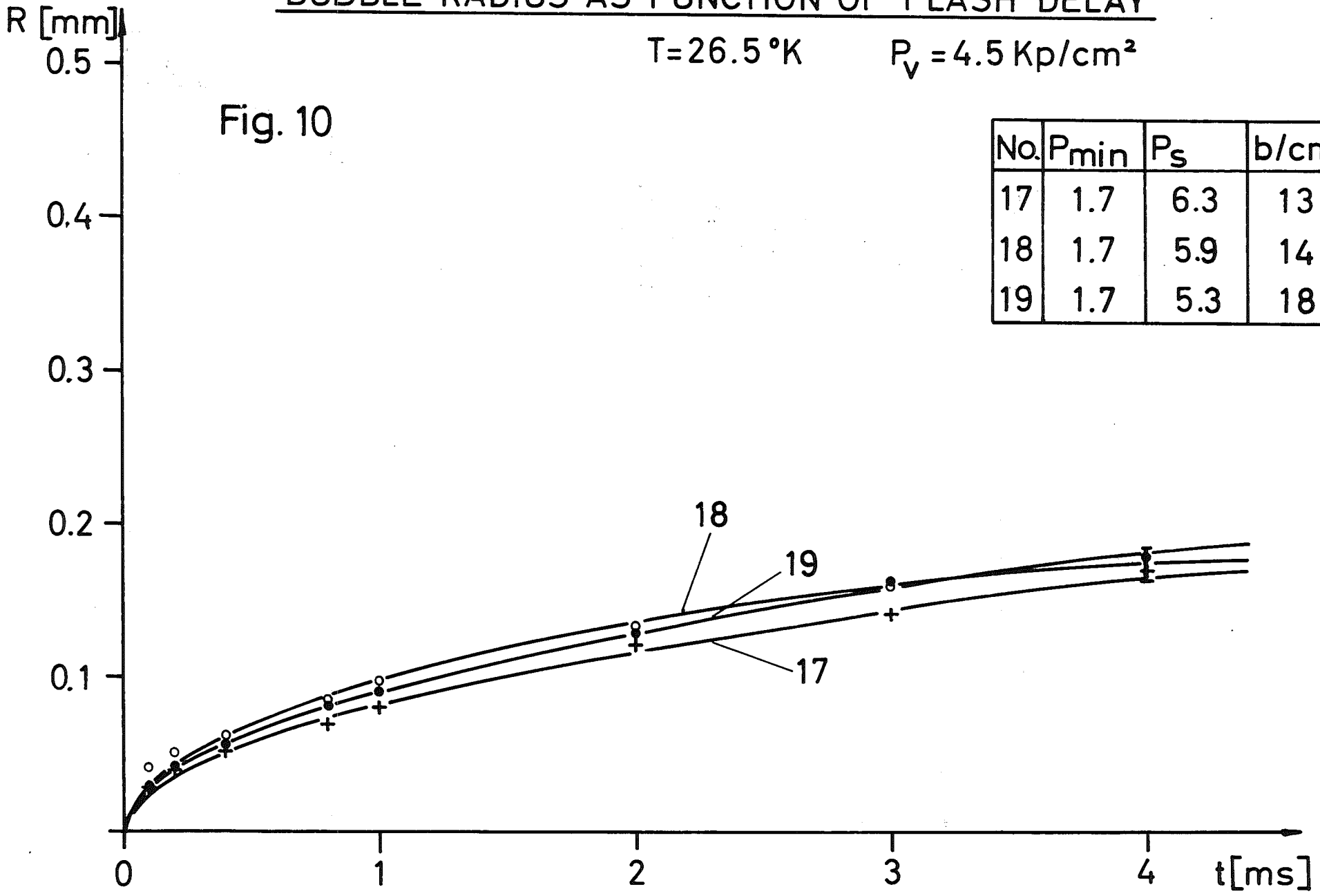

BUBBLE RADIUS AS FUNCTION OF FLASH DELAY

T = 27.0 °K P_v = 5.0 Kp/cm²

Fig. 11

No.	P_{min}	P_s	b/cm
20	2.3	5.9	17
21	2.3	5.3	20
22	2.0	6.5	19

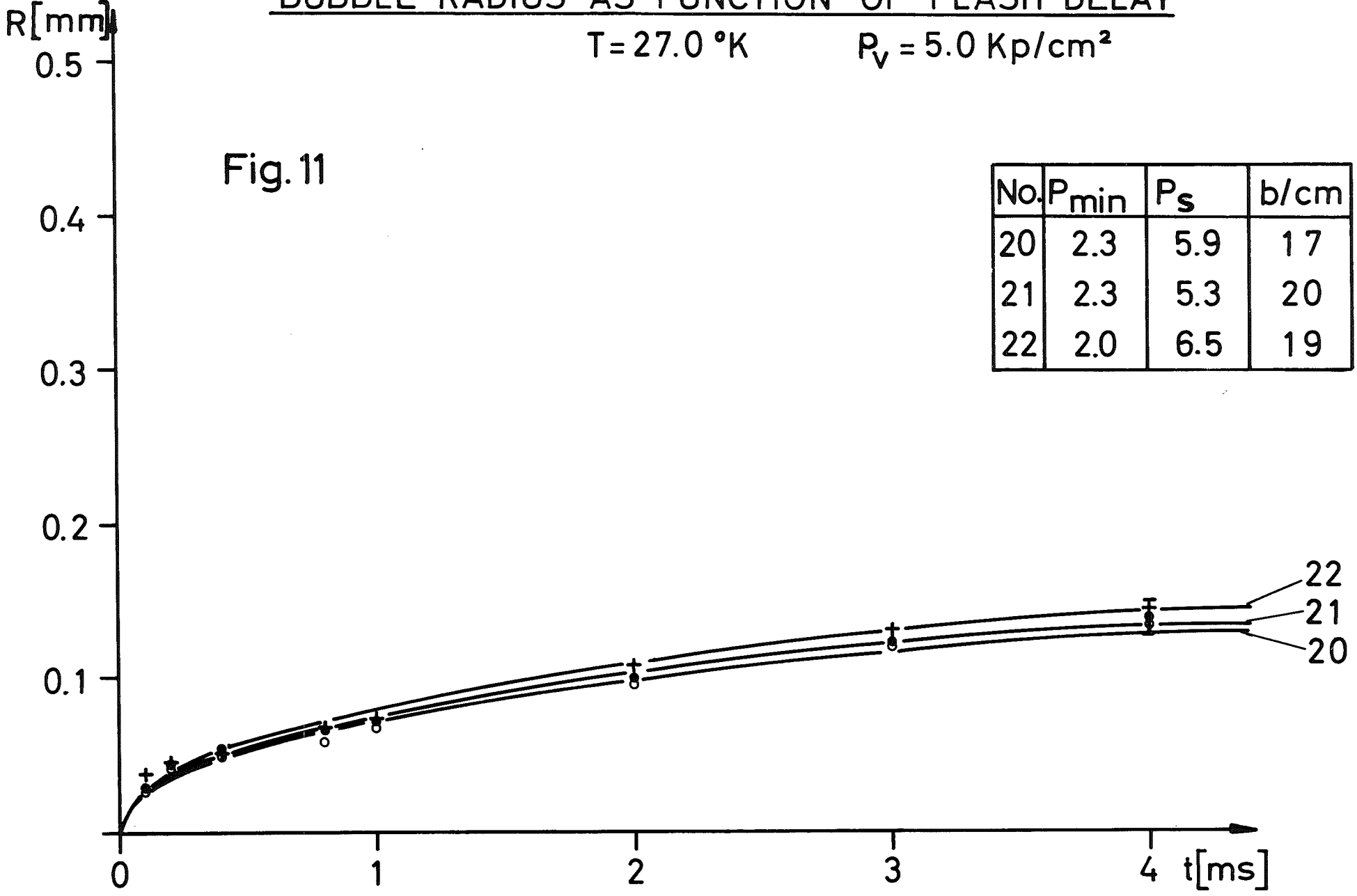

BUBBLE RADIUS AS FUNCTION OF FLASH DELAY

$T = 28.0\ ^{\circ}K$ $\quad P_v = 6.0\ Kp/cm^2$

Fig. 12

No.	P_{min}	P_s	b/cm
23	2.7	6.5	41
24	2.3	6.2	46

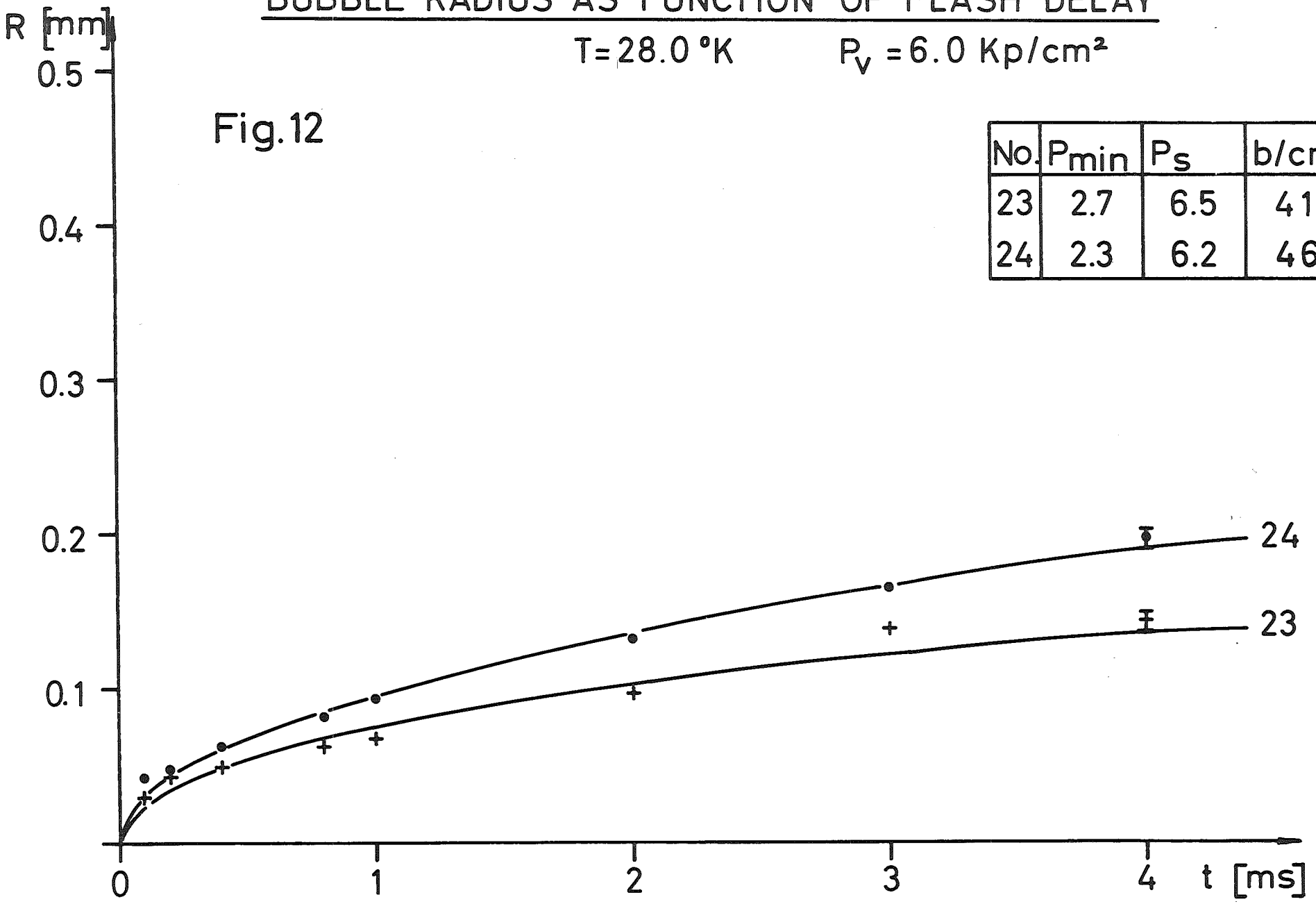

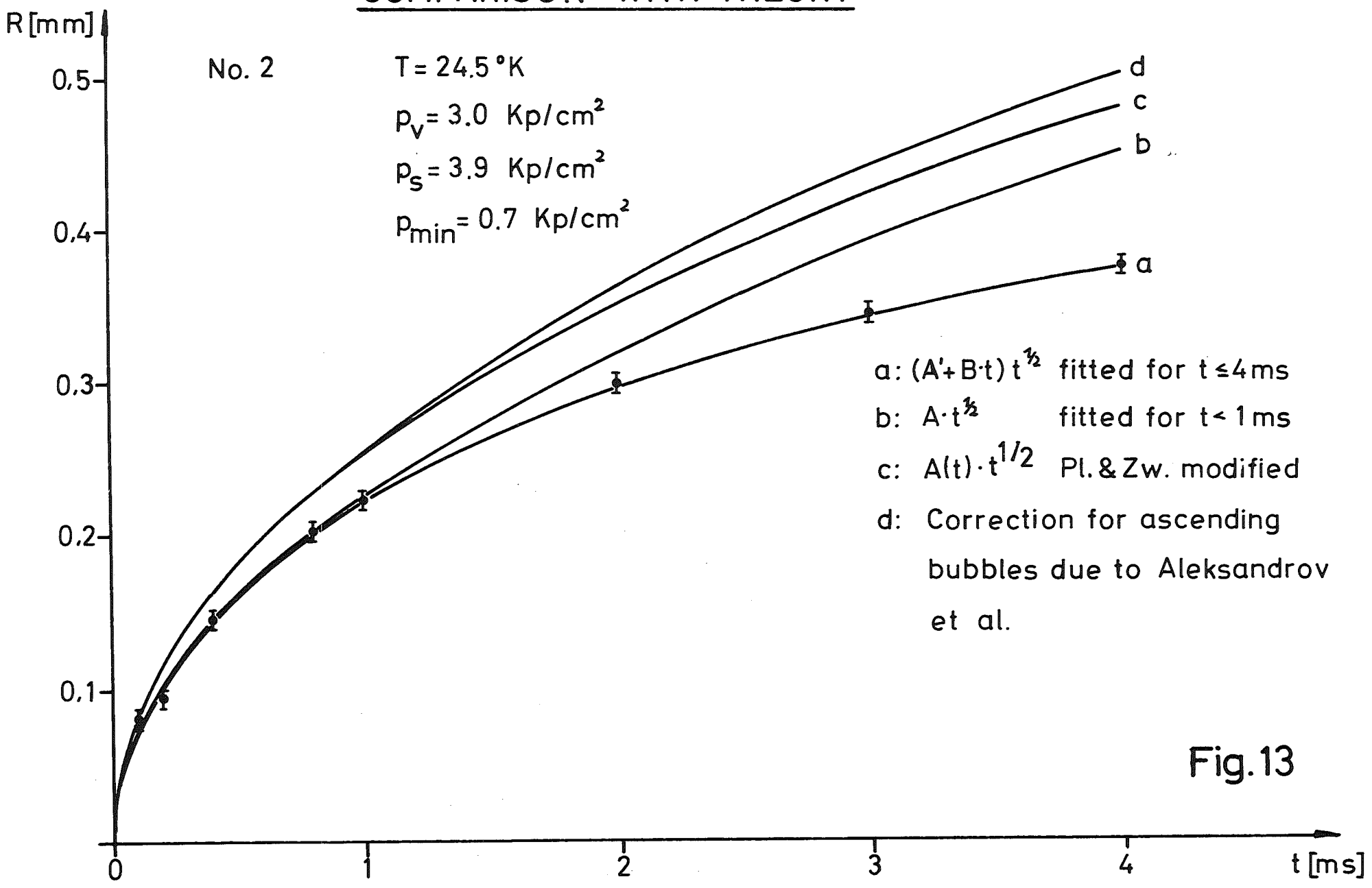
COMPARISON WITH THEORY
R [mm]
No. 2
T = 24.5 °K
p_v = 3.0 Kp/cm²
p_s = 3.9 Kp/cm²
p_{min} = 0.7 Kp/cm²
0,5
0,4
0,3
0,2
0,1
0
1
2
3
4
t [ms]
d
c
b
a
a: $(A'+B\cdot t)\,t^{1/2}$ fitted for t ≤ 4 ms
b: $A\cdot t^{1/2}$ fitted for t < 1 ms
c: $A(t)\cdot t^{1/2}$ Pl. & Zw. modified
d: Correction for ascending bubbles due to Aleksandrov et al.

Fig. 13

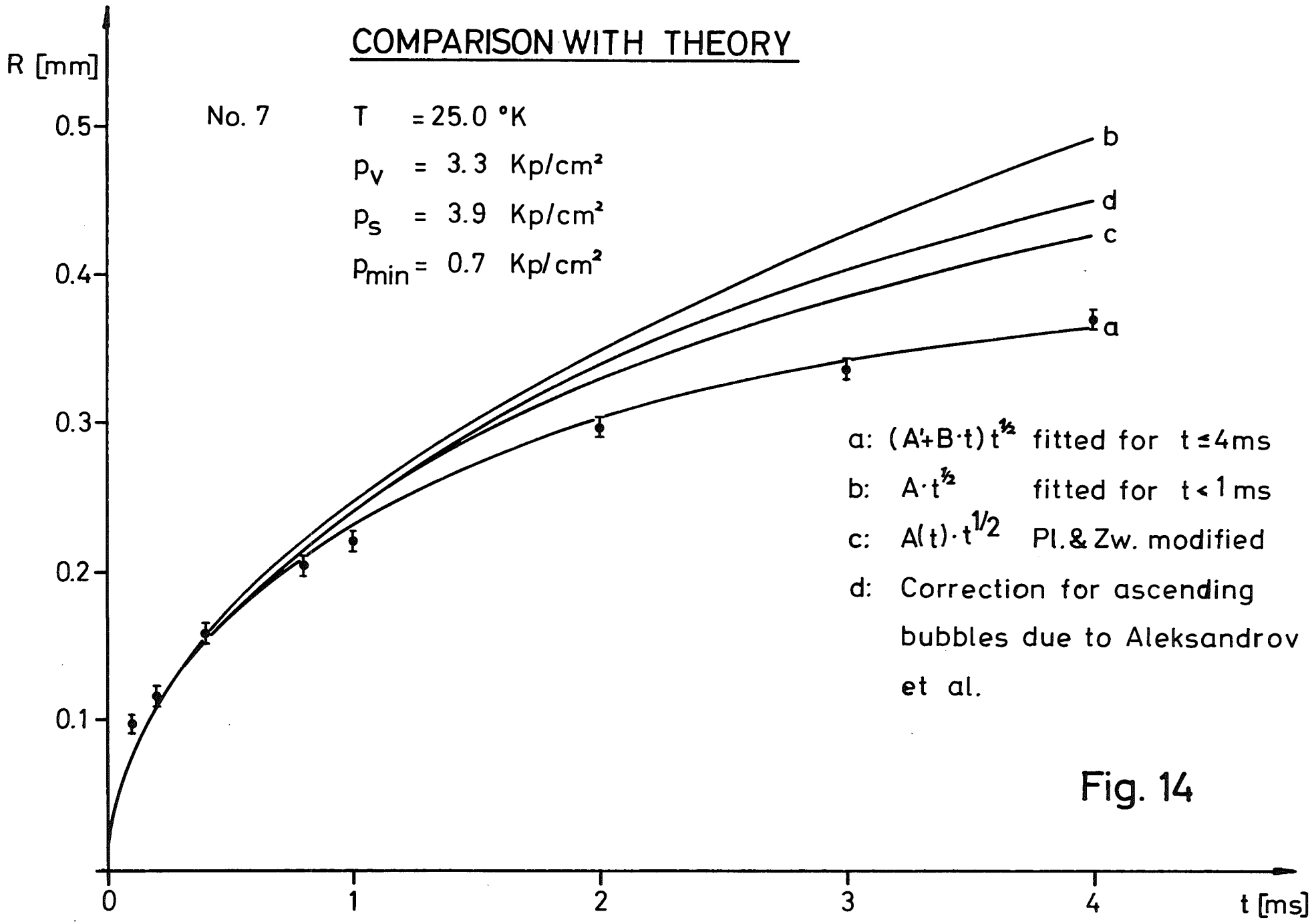
COMPARISON WITH THEORY
R [mm]
No. 7
T = 25.0 °K
p_v = 3.3 Kp/cm²
p_s = 3.9 Kp/cm²
p_{min} = 0.7 Kp/cm²
0.5
0.4
0.3
0.2
0.1
0
1
2
3
4
t [ms]
a
b
c
d
a: $(A'+B\cdot t)\,t^{1/2}$ fitted for $t \leq 4$ ms
b: $A\cdot t^{1/2}$ fitted for $t < 1$ ms
c: $A(t)\cdot t^{1/2}$ Pl. & Zw. modified
d: Correction for ascending bubbles due to Aleksandrov et al.

Fig. 14

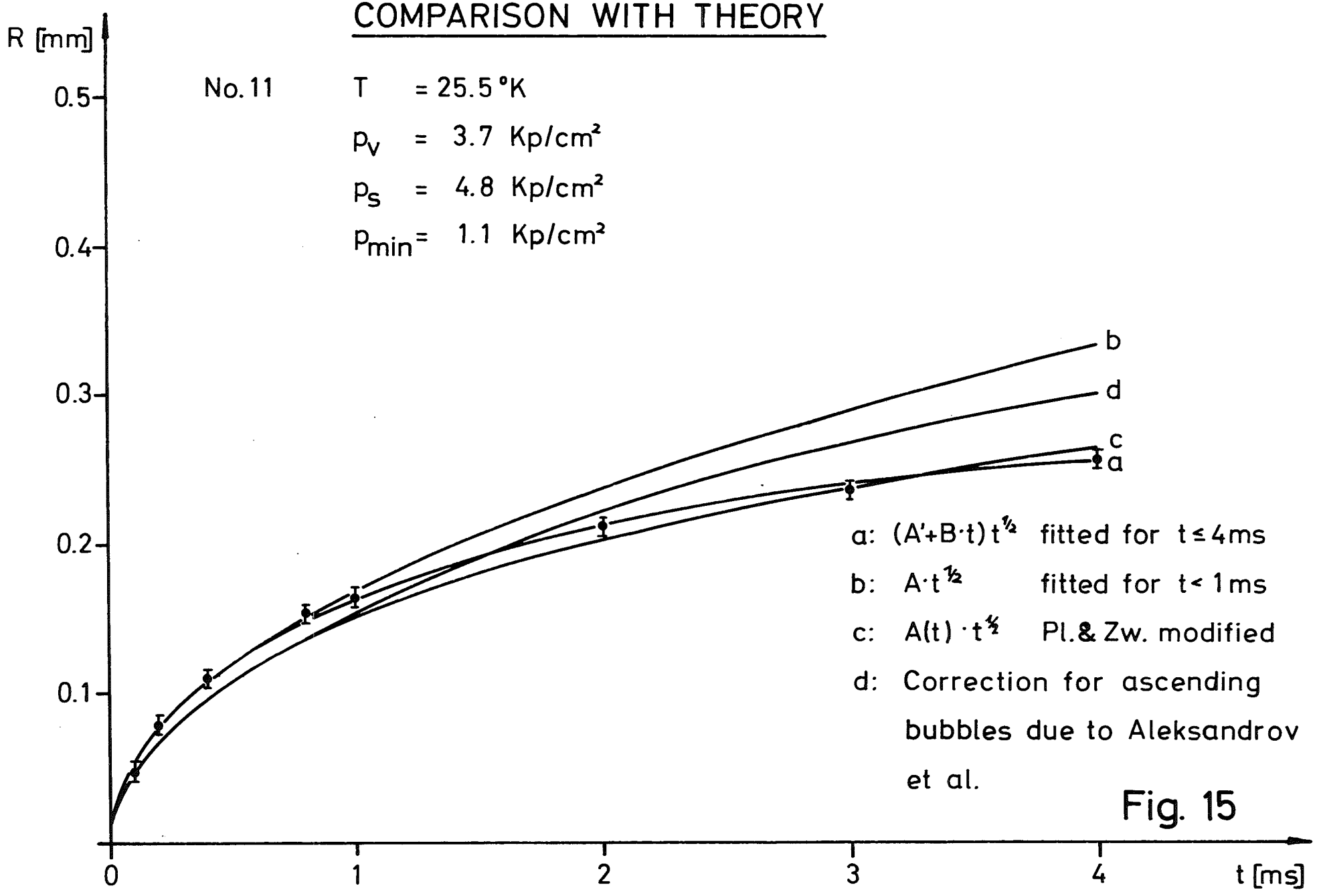
COMPARISON WITH THEORY
R [mm]
No. 11
T = 25.5 °K
p_v = 3.7 Kp/cm²
p_s = 4.8 Kp/cm²
p_{min} = 1.1 Kp/cm²
0.5
0.4
0.3
0.2
0.1
0
1
2
3
4
t [ms]
b
d
c
a
a: $(A'+B\cdot t)\,t^{1/2}$ fitted for $t \leq 4$ms
b: $A\cdot t^{1/2}$ fitted for $t < 1$ms
c: $A(t)\cdot t^{1/2}$ Pl.& Zw. modified
d: Correction for ascending bubbles due to Aleksandrov et al.

Fig. 15

COMPARISON WITH THEORY

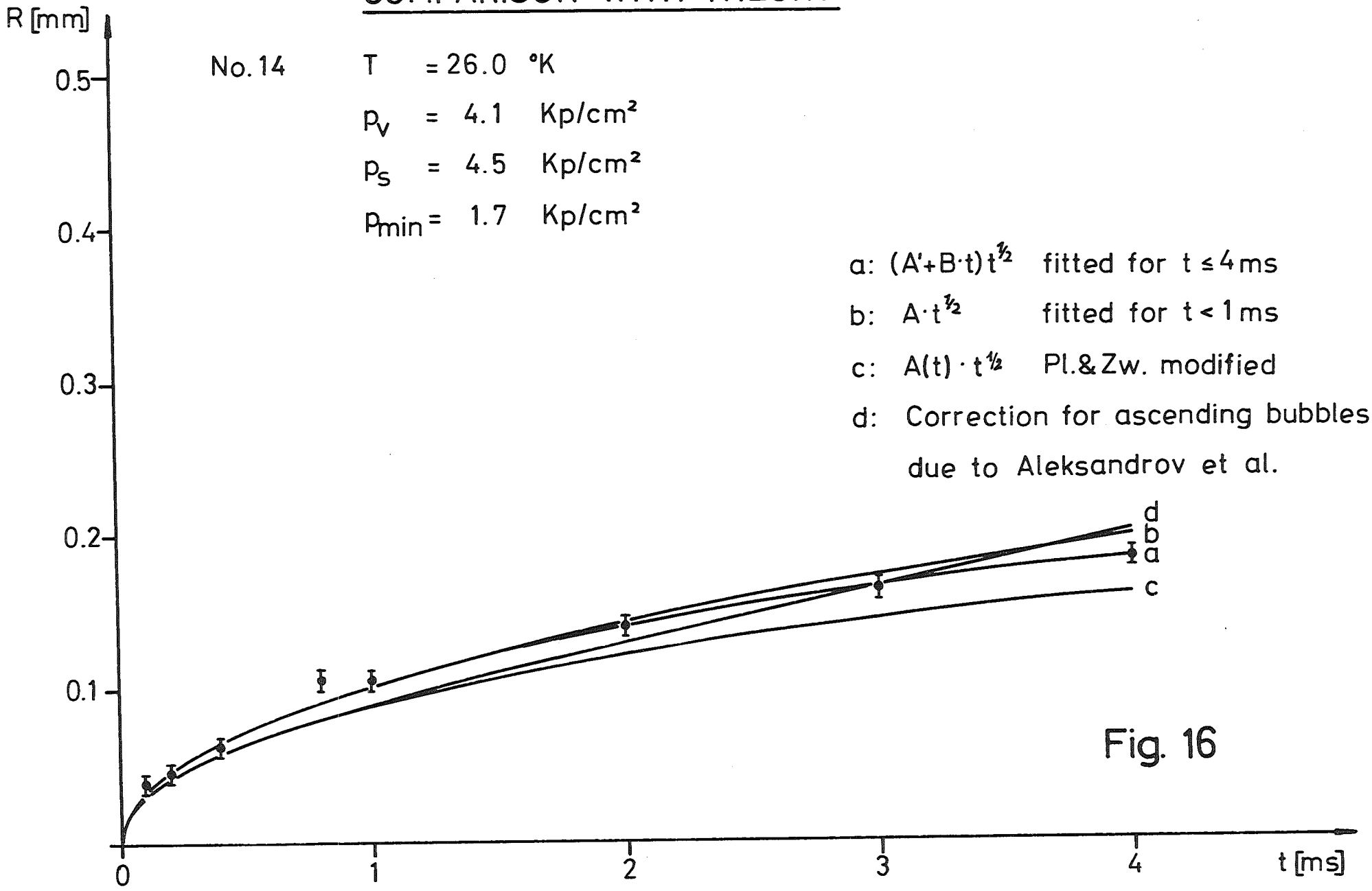

Fig. 16

COMPARISON WITH THEORY

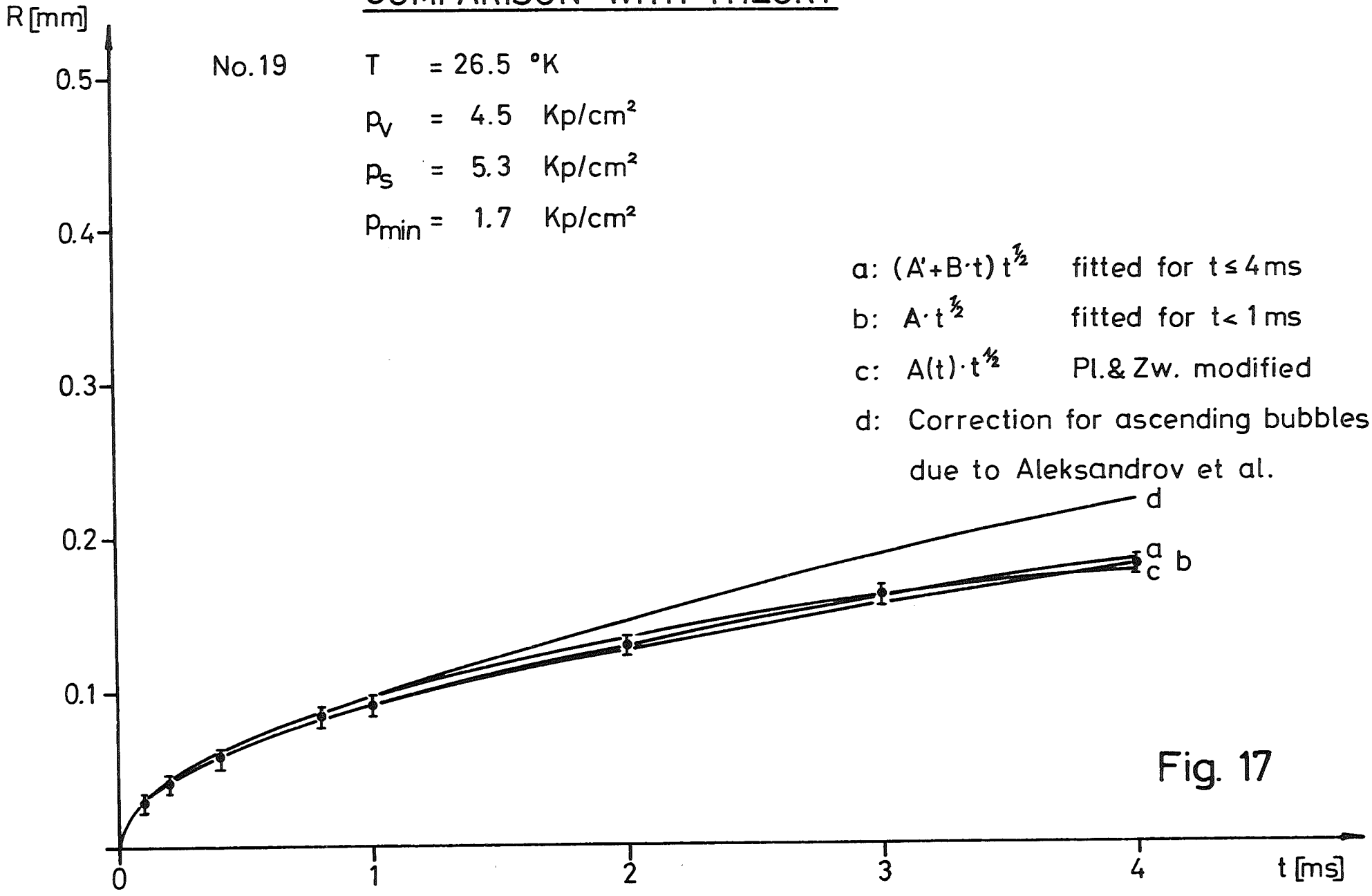

Fig. 17

COMPARISON WITH THEORY

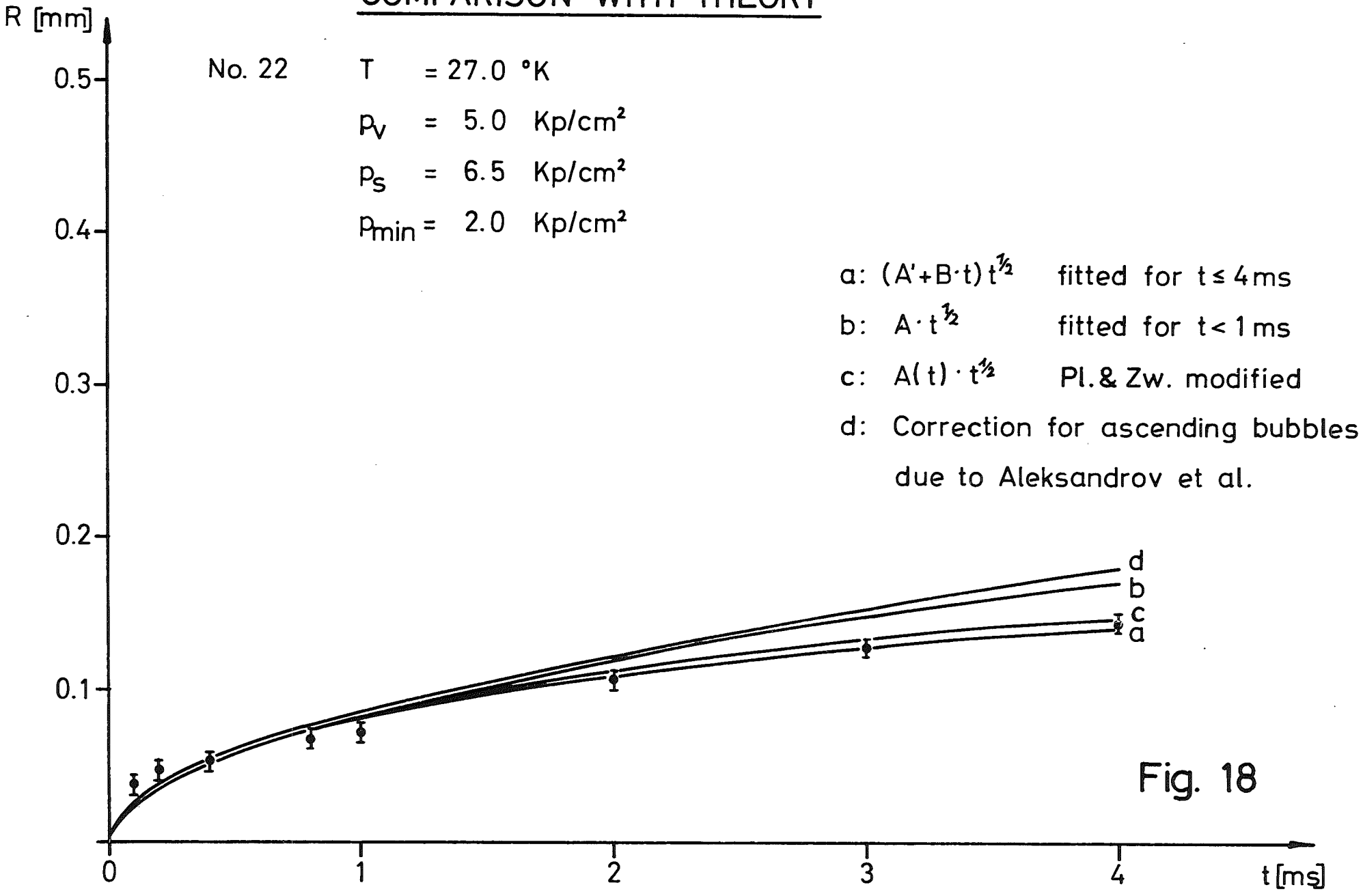

Fig. 18

COMPARISON WITH THEORY

No. 24

$T = 28.0\ ^{\circ}K$

$p_v = 6.0\ Kp/cm^2$

$p_s = 6.2\ Kp/cm^2$

$p_{min} = 2.3\ Kp/cm^2$

a: $(A'+B\cdot t)\,t^{1/2}$ fitted for $t \leq 4$ ms

b: $A\cdot t^{1/2}$ fitted for $t < 1$ ms

c: $A(t)\cdot t^{1/2}$ Pl. & Zw. modified

d: Correction for ascending bubbles due to Aleksandrov et al.

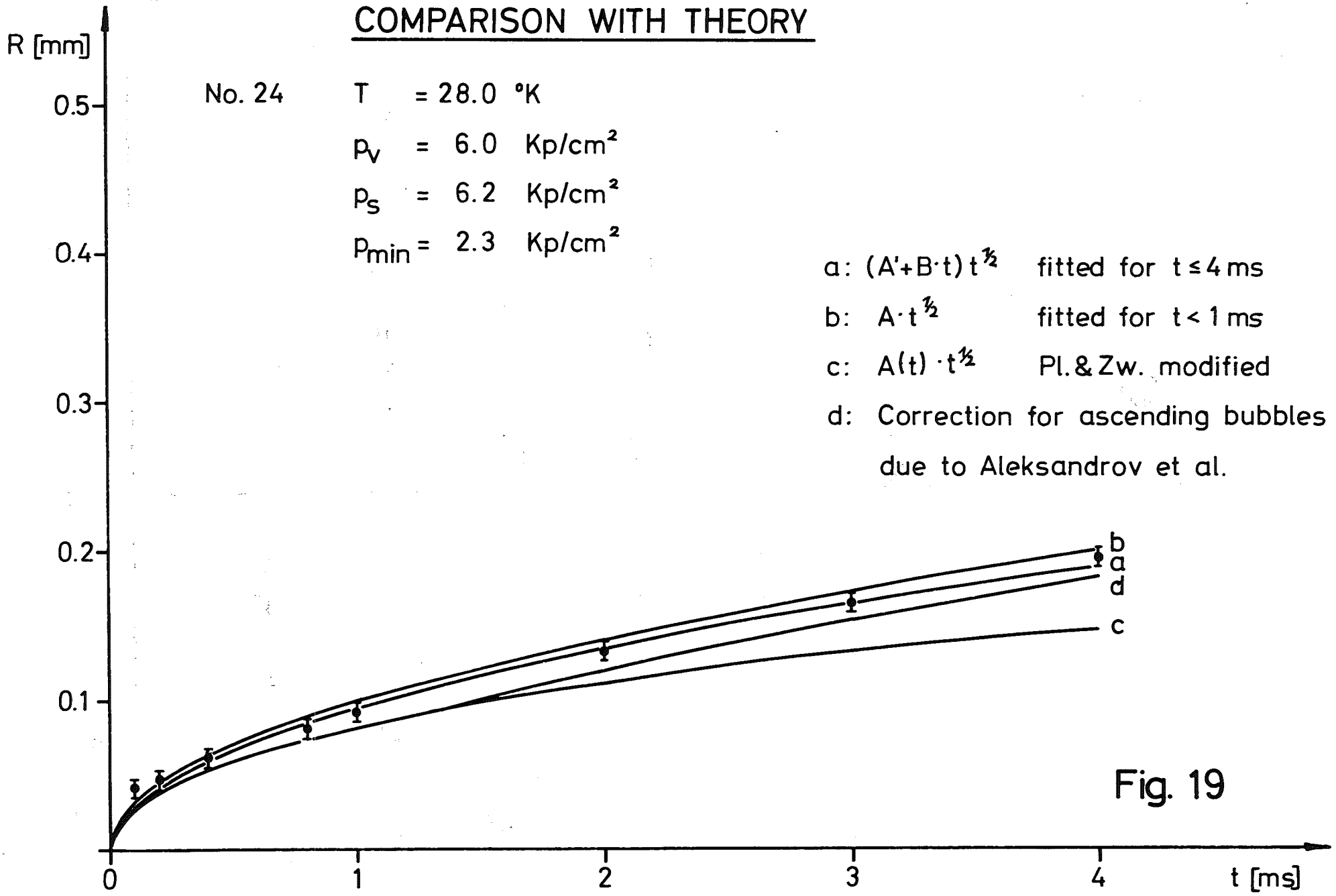

Fig. 19

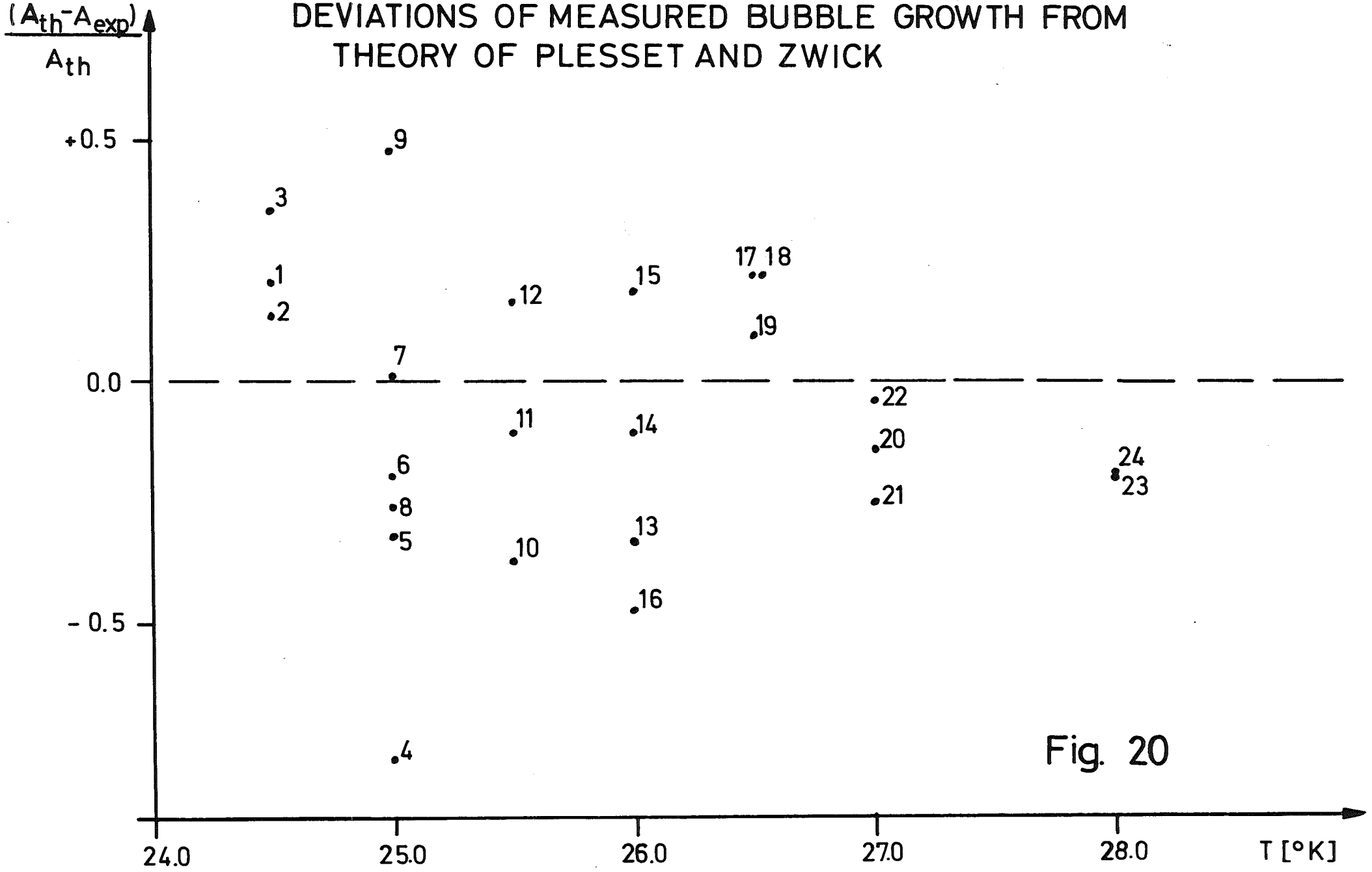
DEVIATIONS OF MEASURED BUBBLE GROWTH FROM THEORY OF PLESSET AND ZWICK
$\frac{(A_{th}-A_{exp})}{A_{th}}$
+0.5
0.0
- 0.5
24.0
25.0
26.0
27.0
28.0
T [°K]
1
2
3
4
5
6
7
8
9
10
11
12
13
14
15
16
17
18
19
20
21
22
23
24

Fig. 20

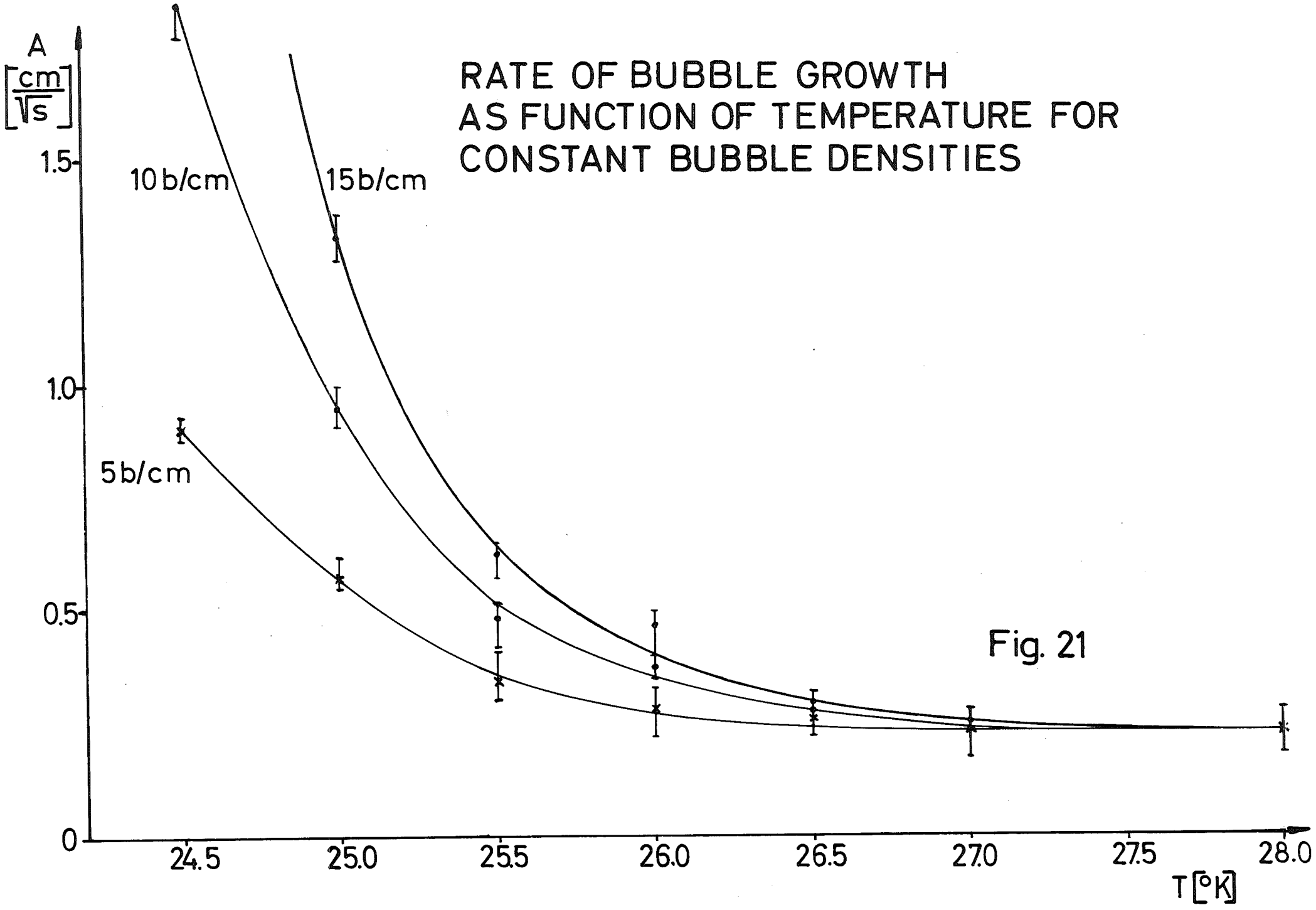
RATE OF BUBBLE GROWTH
AS FUNCTION OF TEMPERATURE FOR
CONSTANT BUBBLE DENSITIES
A
[cm/√s]
1.5
1.0
0.5
0
10 b/cm
15 b/cm
5 b/cm
24.5
25.0
25.5
26.0
26.5
27.0
27.5
28.0
T [°K]

Fig. 21

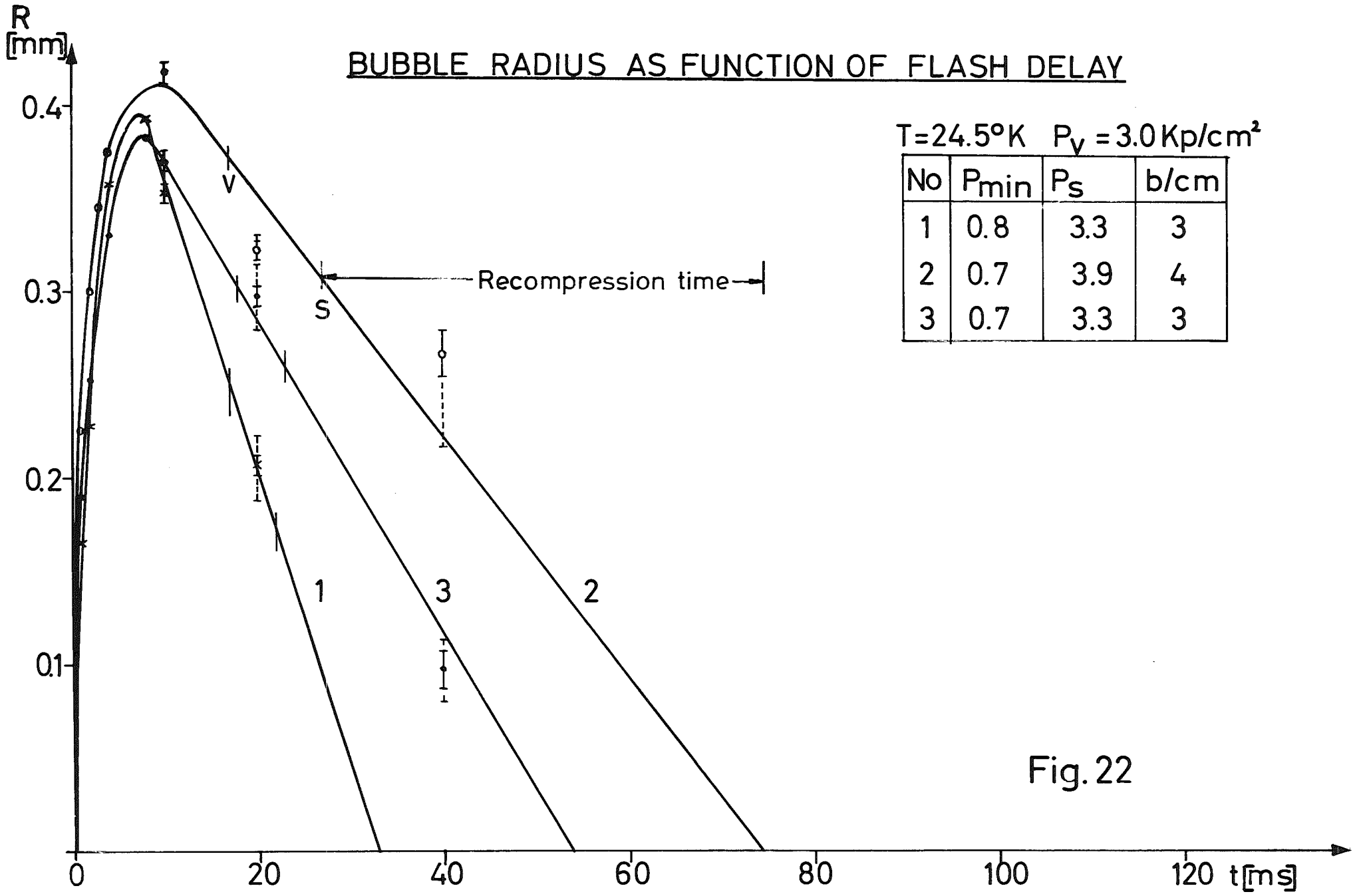

No	P_{min}	P_s	b/cm
1	0.8	3.3	3
2	0.7	3.9	4
3	0.7	3.3	3

Fig. 22

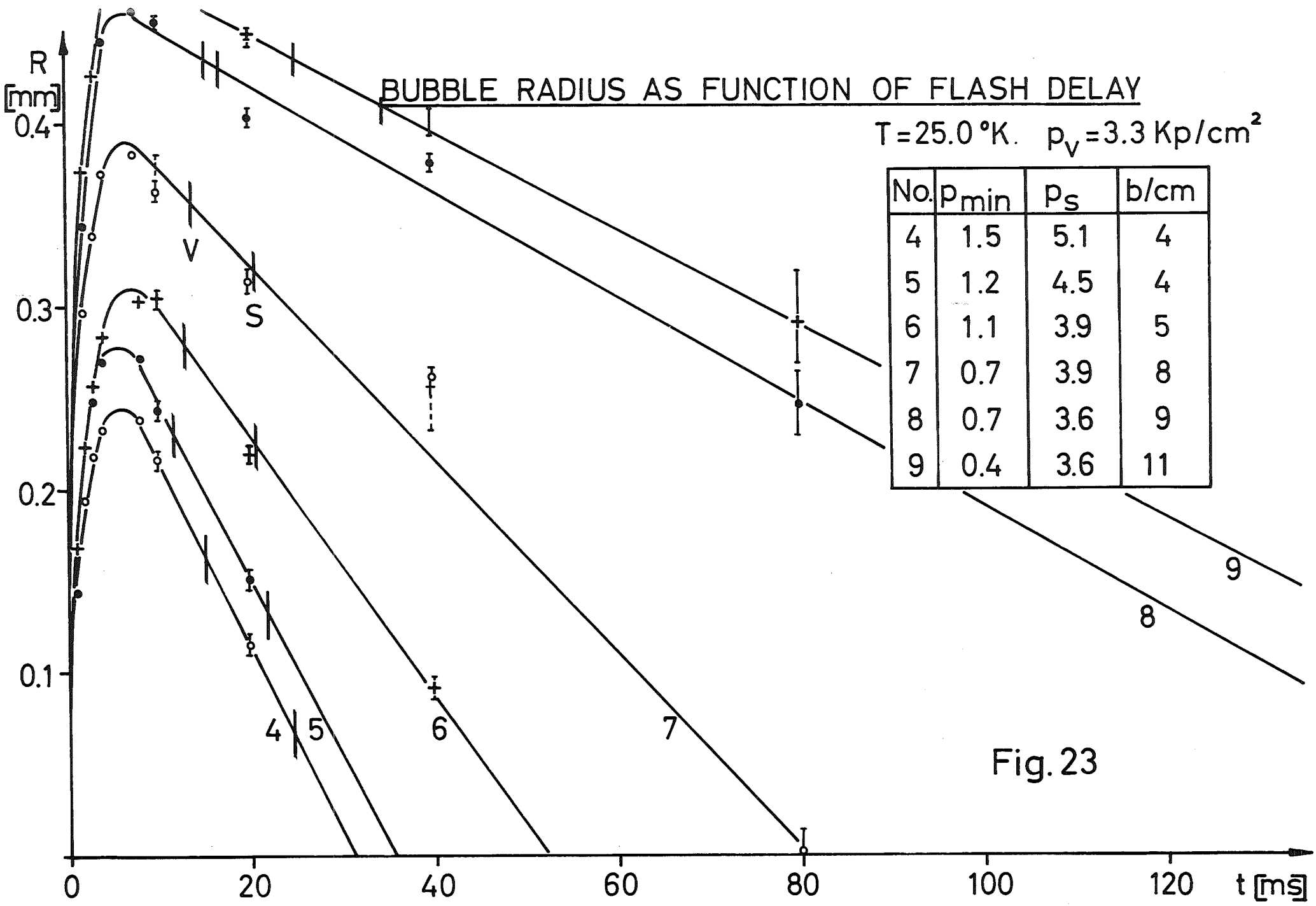

No.	p_{min}	p_s	b/cm
4	1.5	5.1	4
5	1.2	4.5	4
6	1.1	3.9	5
7	0.7	3.9	8
8	0.7	3.6	9
9	0.4	3.6	11

Fig. 23

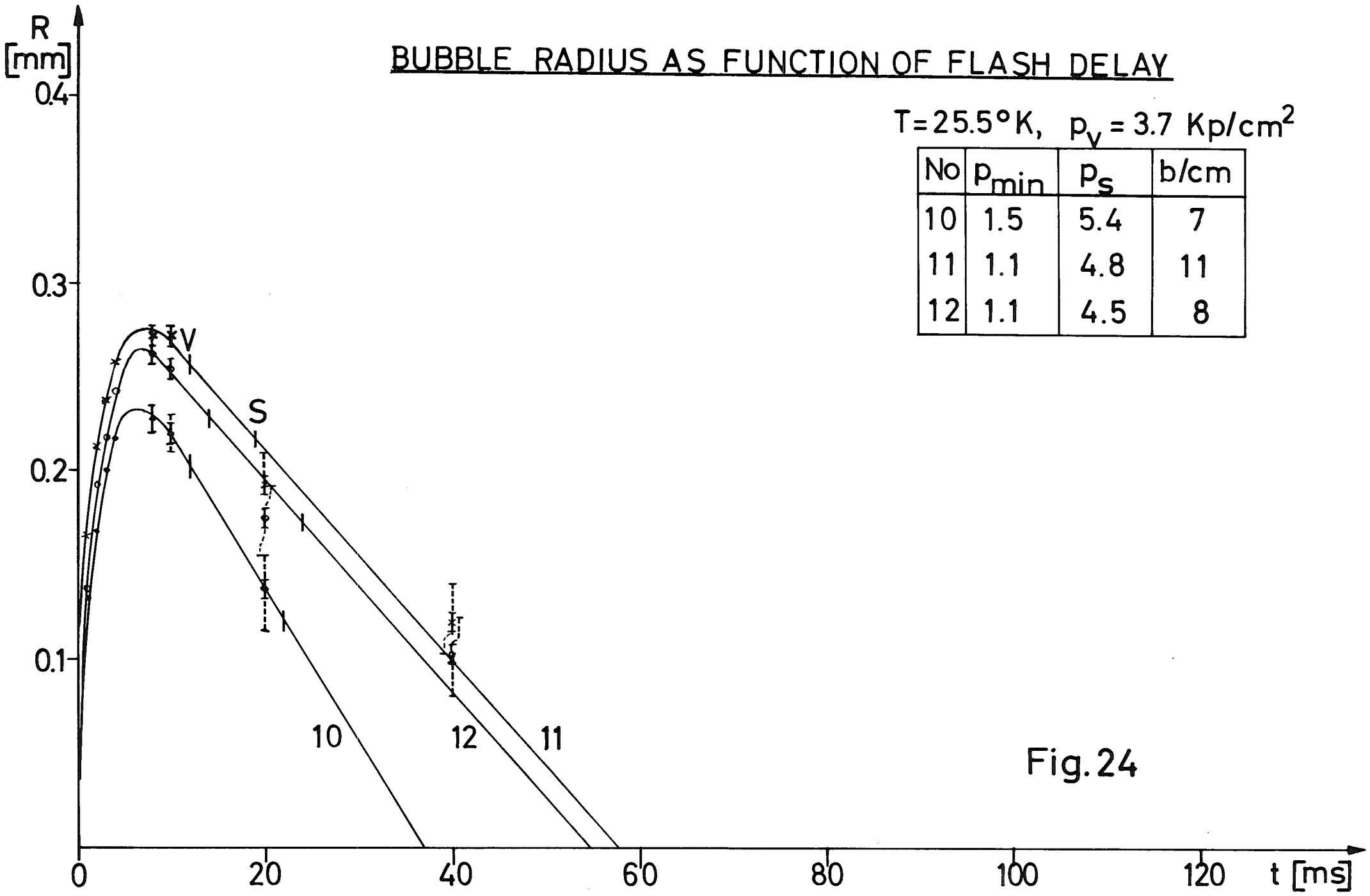

No	p_{min}	p_s	b/cm
10	1.5	5.4	7
11	1.1	4.8	11
12	1.1	4.5	8

Fig. 24

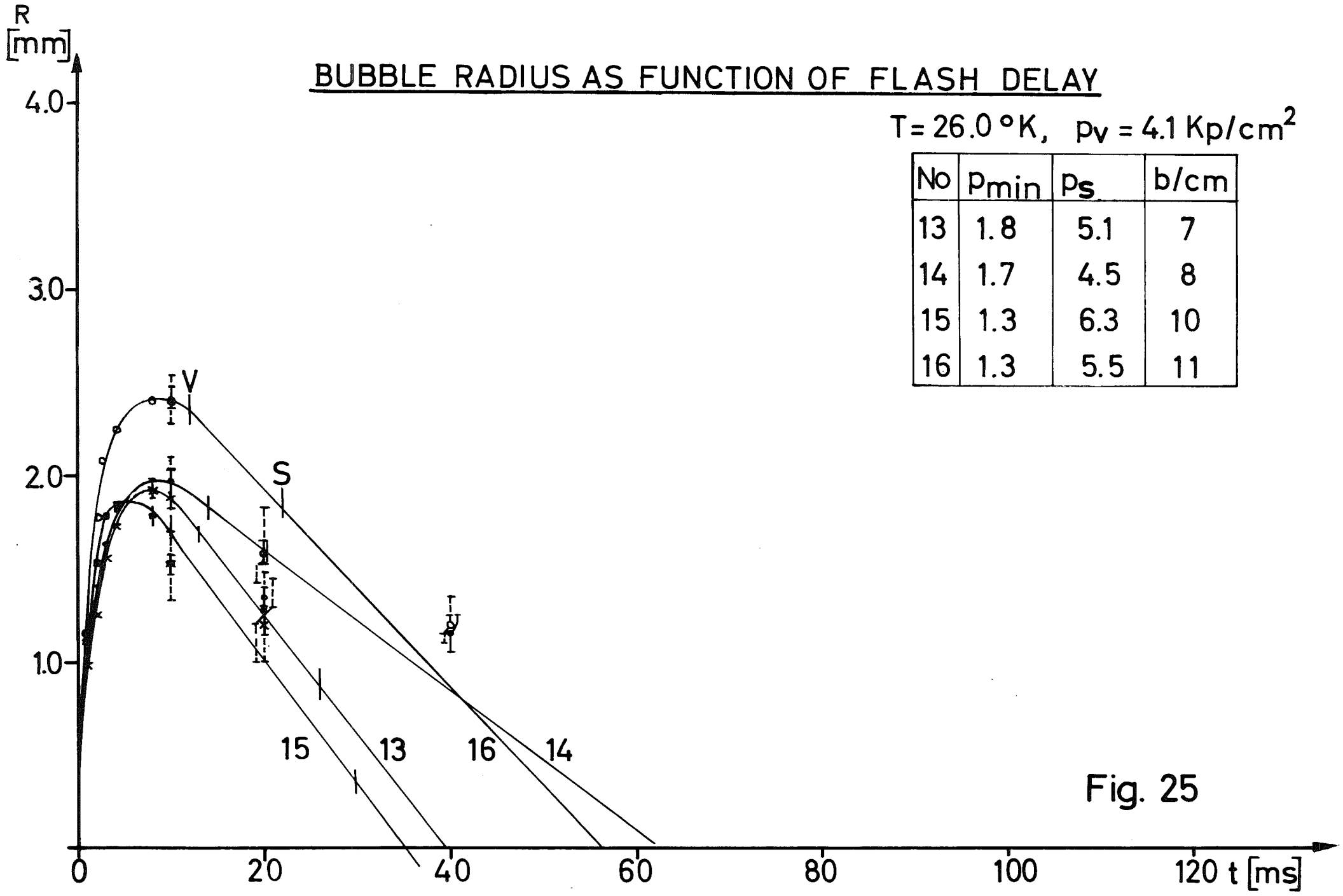

BUBBLE RADIUS AS FUNCTION OF FLASH DELAY

$T = 26.0\,°K$, $p_v = 4.1\ Kp/cm^2$

No	p_{min}	p_s	b/cm
13	1.8	5.1	7
14	1.7	4.5	8
15	1.3	6.3	10
16	1.3	5.5	11

Fig. 25

BUBBLE RADIUS AS FUNCTION OF FLASH DELAY

T = 26.5 °K p_V = 4.5 Kp/cm²

No.	P_{min}	P_s	b/cm
17	1.7	6.3	13
18	1.7	5.9	14
19	1.7	5.3	18

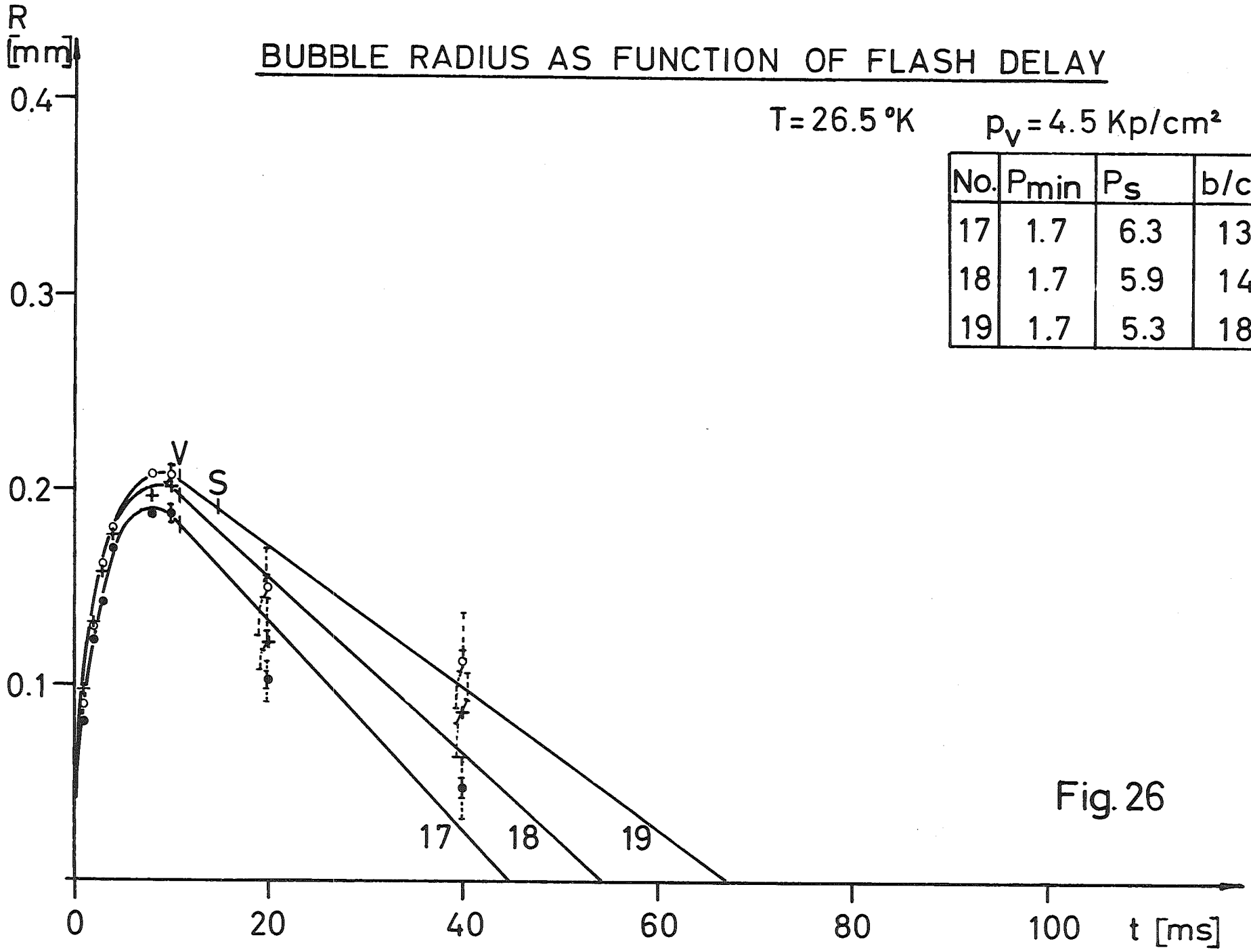

Fig. 26

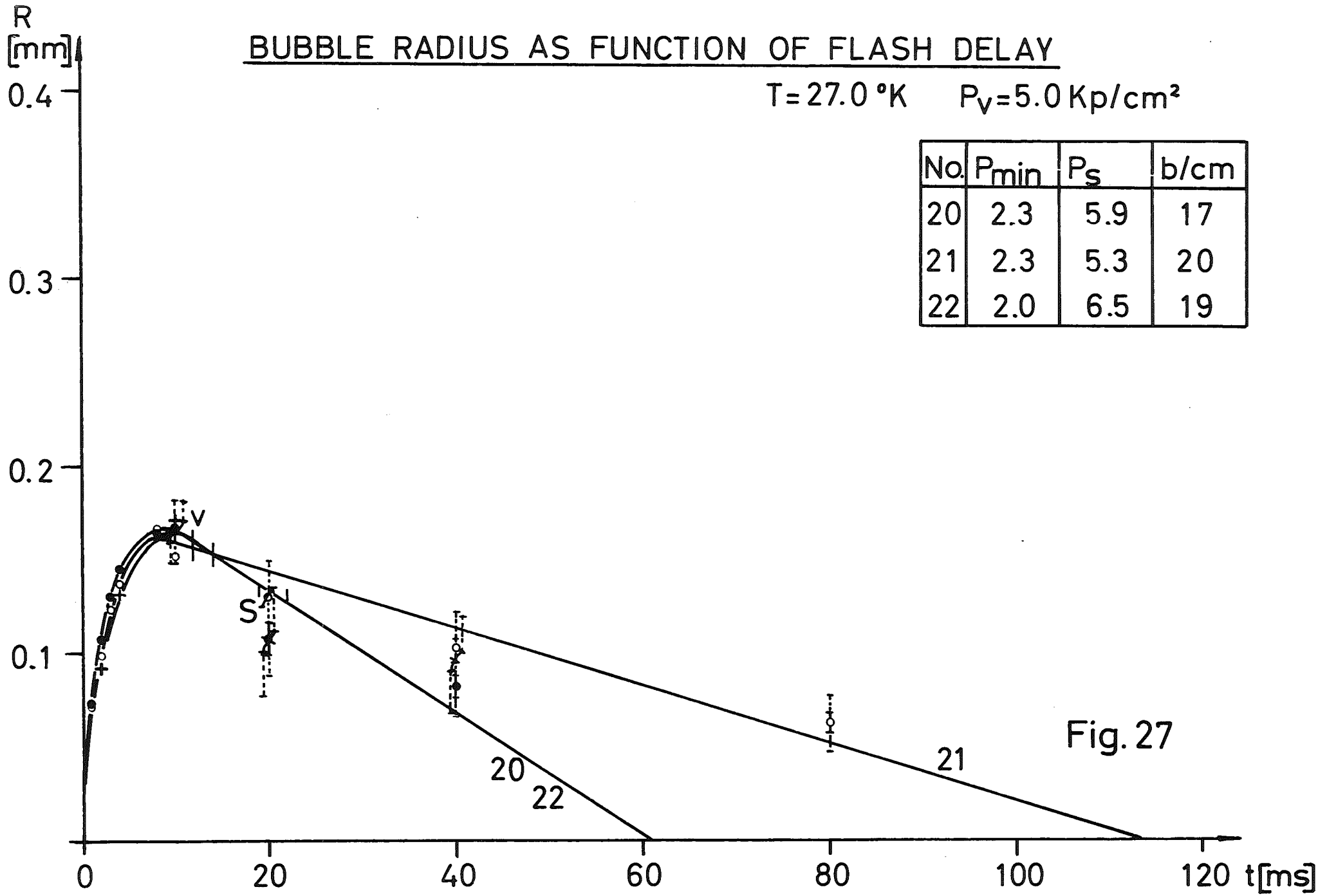

No.	P_{min}	P_s	b/cm
20	2.3	5.9	17
21	2.3	5.3	20
22	2.0	6.5	19

Fig. 27

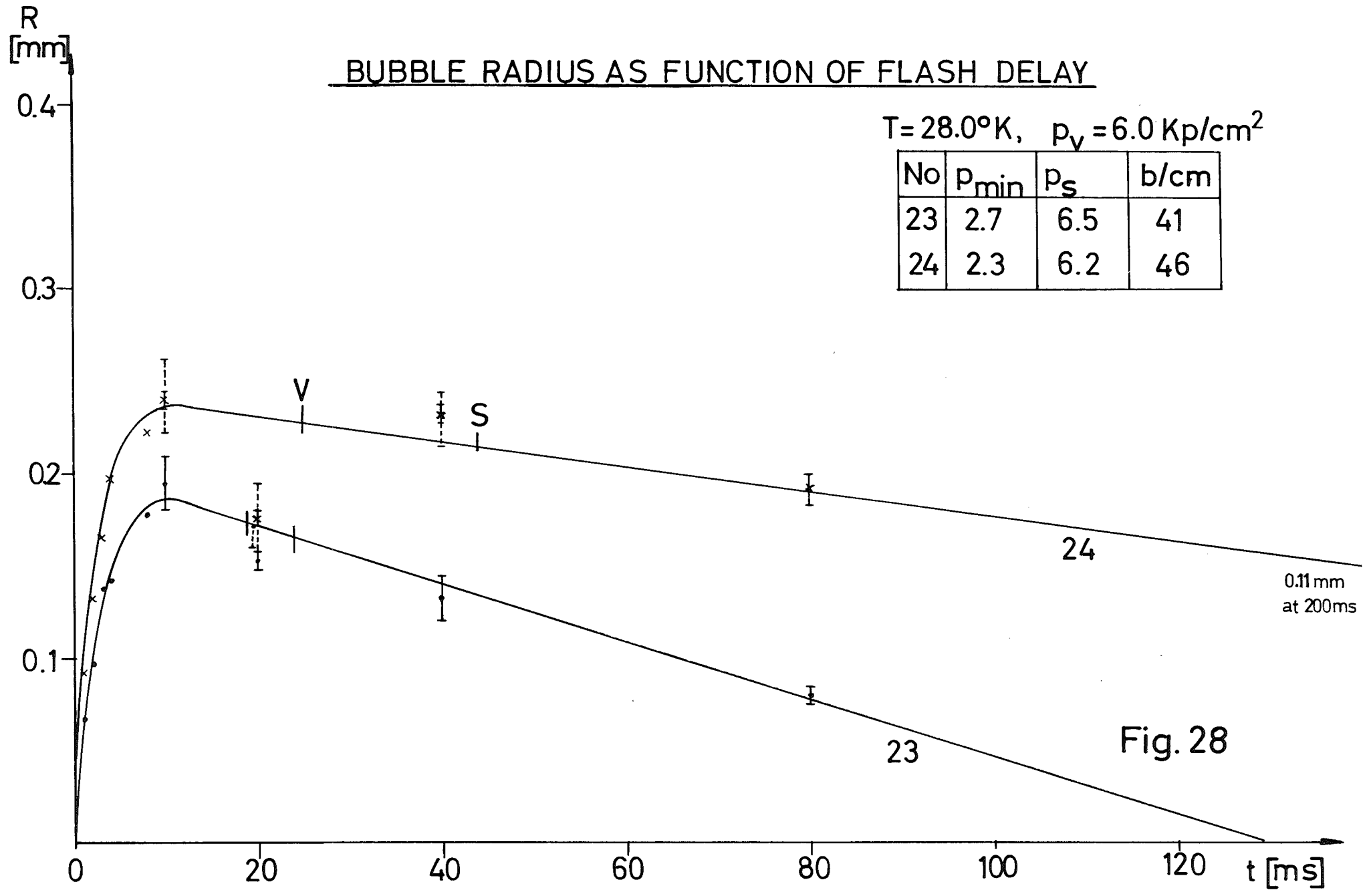
R
[mm]
BUBBLE RADIUS AS FUNCTION OF FLASH DELAY
T= 28.0°K, p_v = 6.0 Kp/cm²
No | p_{min} | p_s | b/cm
23 | 2.7 | 6.5 | 41
24 | 2.3 | 6.2 | 46
0.4
0.3
0.2
0.1
V
S
24
0.11 mm
at 200 ms
23
0
20
40
60
80
100
120
t [ms]

Fig. 28

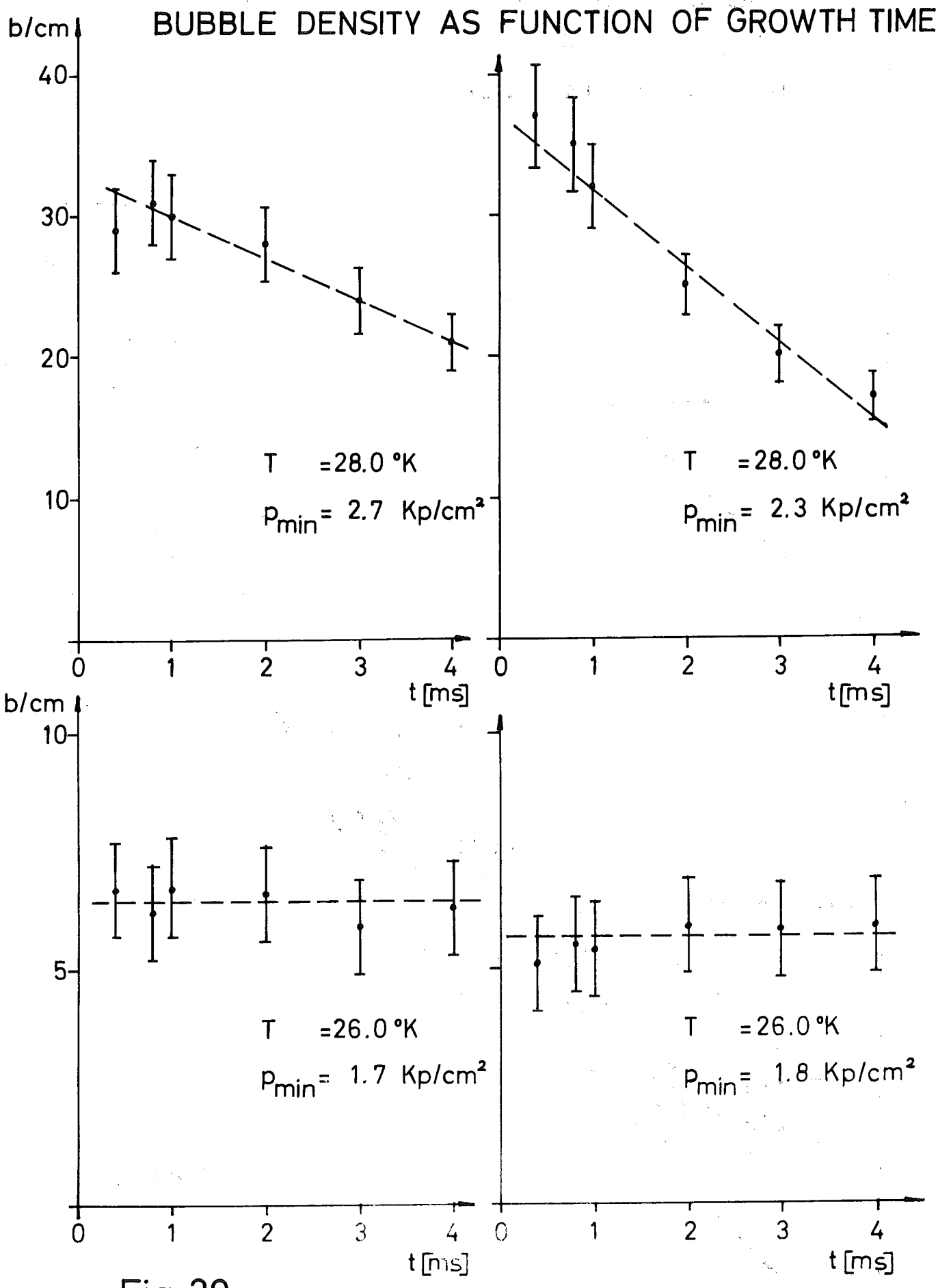
BUBBLE DENSITY AS FUNCTION OF GROWTH TIME
b/cm
40
30
20
10
T =28.0 °K
p_{min} = 2.7 Kp/cm²
T =28.0 °K
p_{min} = 2.3 Kp/cm²
0
1
2
3
4
t [ms]
b/cm
10
5
T =26.0 °K
p_{min} = 1.7 Kp/cm²
T =26.0 °K
p_{min} = 1.8 Kp/cm²
0
1
2
3
4
t [ms]

Fig. 29

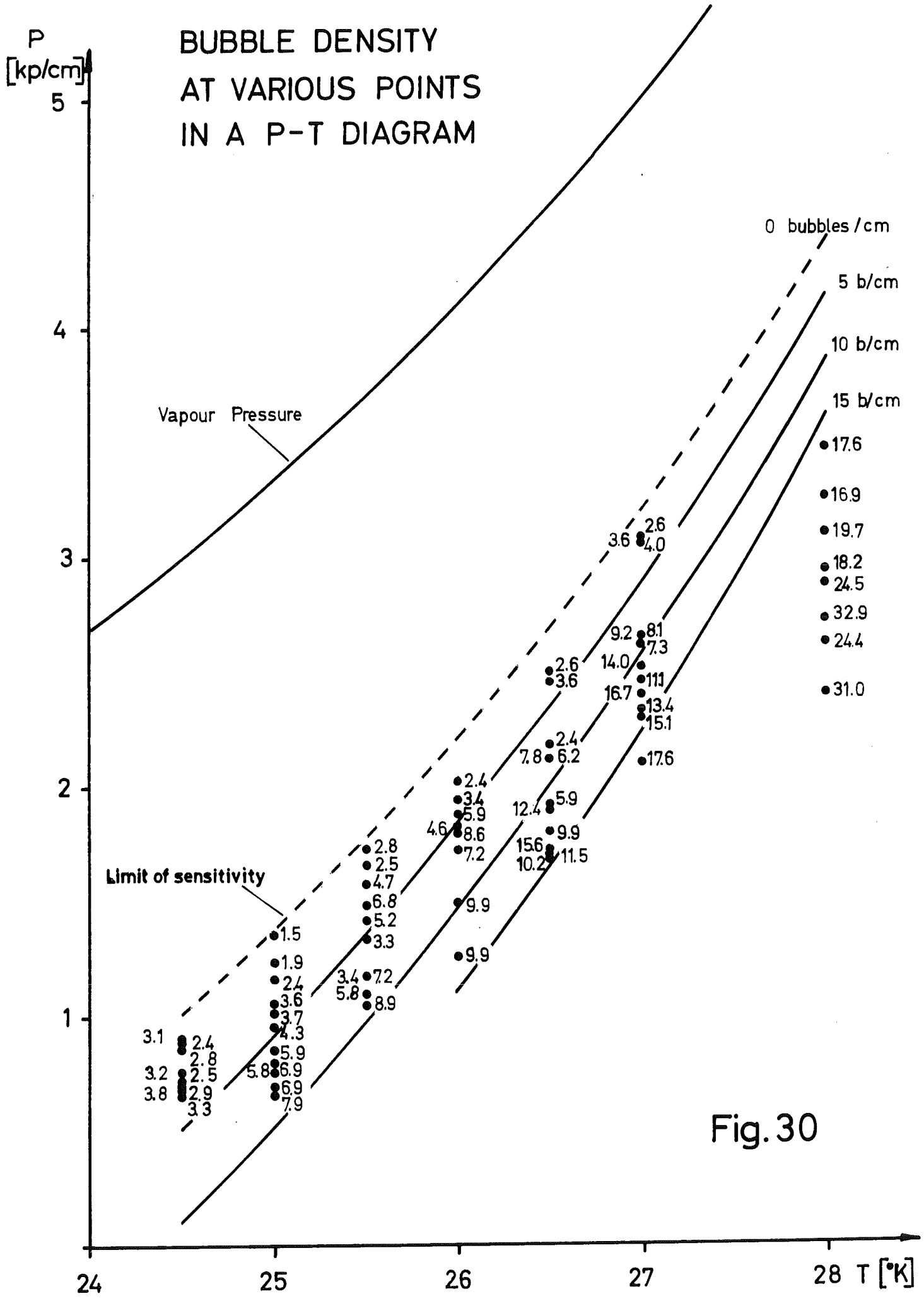
BUBBLE DENSITY
AT VARIOUS POINTS
IN A P-T DIAGRAM
P
[kp/cm]
5
4
3
2
1
Vapour Pressure
Limit of sensitivity
0 bubbles / cm
5 b/cm
10 b/cm
15 b/cm
24
25
26
27
28 T [°K]

Fig. 30

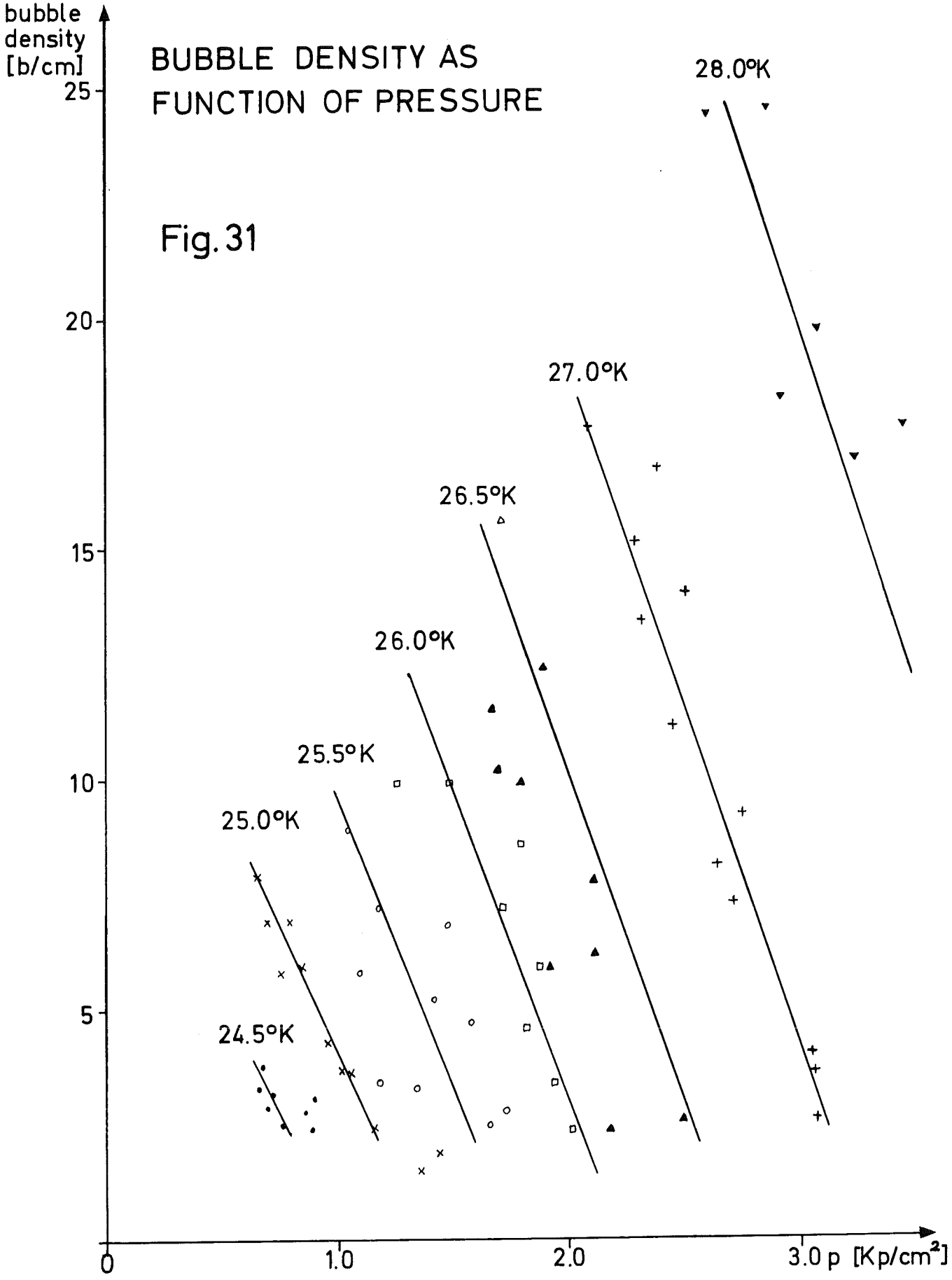
BUBBLE DENSITY AS
FUNCTION OF PRESSURE
Fig. 31
bubble
density
[b/cm]
25
20
15
10
5
0
1.0
2.0
3.0 p [Kp/cm²]
28.0°K
27.0°K
26.5°K
26.0°K
25.5°K
25.0°K
24.5°K